Earth Syst. Sci. Data, 16, 89–120, 2024
https://doi.org/10.5194/essd-16-89-2024

Open Access Earth System Science Data

A synthesis of ocean total alkalinity and dissolved inorganic carbon measurements from 1993 to 2022: the SNAPO-CO2-v1 dataset

Nicolas Metzl[1], Jonathan Fin[1,2], Claire Lo Monaco[1], Claude Mignon[1], Samir Alliouane[3], David Antoine[3,4], Guillaume Bourdin[5], Jacqueline Boutin[1], Yann Bozec[6], Pascal Conan[7,8], Laurent Coppola[3,8], Frédéric Diaz[13,†], Eric Douville[9], Xavier Durrieu de Madron[10], Jean-Pierre Gattuso[3,11], Frédéric Gazeau[3], Melek Golbol[8,12], Bruno Lansard[9], Dominique Lefèvre[13], Nathalie Lefèvre[1], Fabien Lombard[3,14], Férial Louanchi[15], Liliane Merlivat[1], Léa Olivier[1,16], Anne Petrenko[13], Sébastien Petton[17], Mireille Pujo-Pay[7], Christophe Rabouille[9], Gilles Reverdin[1], Céline Ridame[1], Aline Tribollet[1], Vincenzo Vellucci[8,12], Thibaut Wagener[13], and Cathy Wimart-Rousseau[13,18]

[1]Laboratoire LOCEAN/IPSL, Sorbonne Université-CNRS-IRD-MNHN, 75005 Paris, France
[2]OSU Ecce Terra, Sorbonne Université-CNRS, 75005 Paris, France
[3]CNRS, Laboratoire d'Océanographie de Villefranche, LOV, Sorbonne Université, 06230 Villefranche-sur-Mer, France
[4]Remote Sensing and Satellite Research Group, School of Earth and Planetary Sciences, Curtin University, Perth, WA 6845, Australia
[5]School of Marine Sciences, University of Maine, 04469 Orono, USA
[6]Station Biologique de Roscoff, UMR 7144 – EDYCO-CHIMAR, 29680 Roscoff, France
[7]CNRS, Laboratoire d'Océanographie Microbienne, LOMIC, Sorbonne Université, 66650 Banyuls-sur-Mer, France
[8]CNRS, OSU Station Marines, STAMAR, Sorbonne Université, 75006 Paris, France
[9]Laboratoire des Sciences du Climat et de l'Environnement, LSCE/IPSL, UMR 8212 CEA-CNRS-UVSQ, Universiteì Paris-Saclay, 91191 Gif-sur-Yvette, France
[10]CEFREM, CNRS-Université de Perpignan Via Domitia, 66860 Perpignan, France
[11]Institute for Sustainable Development and International Relations, Sciences Po, 75007 Paris, France
[12]CNRS, Institut de la Mer de Villefranche, IMEV, Sorbonne Université, 06230 Villefranche-sur-Mer, France
[13]Aix Marseille University, Université de Toulon, CNRS, IRD, MIO, 13288 Marseille, France
[14]Research Federation for the study of Global Ocean Systems Ecology and Evolution, FR2022/Tara GOSEE, 75000 Paris, France
[15]CVRM: Laboratoire de Conservation et de Valorisation des Ressources Marines, Ecole Nationale Supérieure des Sciences de la Mer et de l'Aménagement du Littoral (ENSSMAL), Station de recherche de Sidi Fredj, 16320 Alger, Algeria
[16]Alfred Wegener Institute, Helmholtz Centre for Polar and Marine Research, 27515 Bremerhaven, Germany
[17]Ifremer, Brest University, CNRS, IRD, LEMAR, 29840 Argenton, France
[18]GEOMAR Helmholtz Center for Ocean Research Kiel, Helmholtz Association of German Research Centres, 24105 Kiel, Germany
†deceased, 14 March 2021

Correspondence: Nicolas Metzl (nicolas.metzl@locean.ipsl.fr)

Received: 30 July 2023 – Discussion started: 16 August 2023
Revised: 18 October 2023 – Accepted: 17 November 2023 – Published: 9 January 2024

Published by Copernicus Publications.

Abstract. Total alkalinity (A_T) and dissolved inorganic carbon (C_T) in the oceans are important properties with respect to understanding the ocean carbon cycle and its link to global change (ocean carbon sinks and sources, ocean acidification) and ultimately finding carbon-based solutions or mitigation procedures (marine carbon removal). We present a database of more than 44 400 A_T and C_T observations along with basic ancillary data (spatiotemporal location, depth, temperature and salinity) from various ocean regions obtained, mainly in the framework of French projects, since 1993. This includes both surface and water column data acquired in the open ocean, coastal zones and in the Mediterranean Sea and either from time series or dedicated one-off cruises. Most A_T and C_T data in this synthesis were measured from discrete samples using the same closed-cell potentiometric titration calibrated with Certified Reference Material, with an overall accuracy of $\pm 4\,\mu mol\,kg^{-1}$ for both A_T and C_T. The data are provided in two separate datasets – for the Global Ocean and the Mediterranean Sea (https://doi.org/10.17882/95414, Metzl et al., 2023), respectively – that offer a direct use for regional or global purposes, e.g., A_T–salinity relationships, long-term C_T estimates, and constraint and validation of diagnostic C_T and A_T reconstructed fields or ocean carbon and coupled climate–carbon models simulations as well as data derived from Biogeochemical-Argo (BGC-Argo) floats. When associated with other properties, these data can also be used to calculate pH, the fugacity of CO_2 (fCO_2) and other carbon system properties to derive ocean acidification rates or air–sea CO_2 fluxes.

1 Introduction

Since 1750, humans activities have added 700 (±75) PgC of anthropogenic carbon dioxide to the atmosphere by burning fossil fuels, producing cement and changing land use (Friedlingstein et al., 2022), thereby driving up the atmospheric carbon dioxide (CO_2) level and leading to unequivocal global change. The ocean plays a major role in reducing the impact of climate change by absorbing more than 90 % of the excess heat in the climate system (Cheng et al., 2020; von Schuckmann et al., 2020, 2023; IPCC, 2022) and about 25 % of anthropogenic CO_2 (Friedlingstein et al., 2022). However, oceanic CO_2 uptake changes the chemistry of seawater, reducing its buffering capacity (Revelle and Suess, 1957; Jiang et al., 2023a) and leading to a process known as "ocean acidification", with potential impacts on marine organisms (Fabry et al., 2008; Doney et al., 2009, 2020; Gattuso et al., 2015). Along with atmospheric CO_2 concentrations, surface-ocean temperature, ocean heat content, sea level, sea ice and glaciers, ocean acidification (a decrease in pH) is now recognized by the World Meteorological Organization (WMO) as one of the seven key global climate indicators (WMO, 2018). In the framework of the 2030 Agenda for Sustainable Development, the United Nations established a set of Sustainable Development Goals (SDGs; United Nations, 2020), including a goal dedicated to the ocean (SDG 14, "Life below water") which calls for work to "conserve and sustainably use the oceans, seas and marine resources for sustainable development". Ocean acidification is specifically referred in the SDG indicator 14.3.1 coordinated by the Intergovernmental Oceanographic Commission (IOC) of the United Nations Educational, Scientific and Cultural Organization (UNESCO). Observing the carbonate system in the oceans and marginal seas and understanding how this system changes over time is, thus, highly relevant not only to quantify the Global Ocean carbon budget, the anthropogenic CO_2 inventories or ocean acidification rates but also to understand and simulate the processes that govern the complex CO_2 cycle in the ocean and to better predict the future evolution of climate and global changes (Eyring et al., 2016; Kwiatkowski et al., 2020; Jiang et al., 2023a).

The number and quality of ocean CO_2 fugacity (fCO_2), total alkalinity (A_T), dissolved inorganic carbon (C_T) and pH measurements have increased substantially over the past few decades. Quality-controlled observations are now regularly assembled in global data syntheses such as SOCAT (Surface Ocean CO_2 Atlas; Pfeil et al., 2013; Bakker et al., 2014, 2016) and GLODAP (Global Ocean Data Analysis Project; Key et al., 2004; Olsen et al., 2016, 2019, 2020; Lauvset et al., 2021, 2022). These datasets allow for the evaluation of properties' trends in the Global Ocean, including the change in the ocean CO_2 sink (e.g., Wanninkhof et al., 2013; Friedlingstein et al., 2022; Watson et al., 2020), anthropogenic CO_2 inventories (e.g., Sabine et al., 2004; Khatiwala et al., 2013; Gruber et al., 2019) and ocean acidification (Lauvset et al., 2015, 2020; Jiang et al., 2019; Feely et al., 2023; Ma et al., 2023). Thanks to publicly available, consistent and quality-controlled databases, new methods have been recently developed (Carter et al., 2016; Sauzède et al., 2017; Bittig et al., 2018) to reproduce A_T and C_T distributions from other properties, like temperature, salinity and oxygen, that are more often observed in the water column, especially by autonomous floats (Claustre et al., 2020; Mignot et al., 2023). These methods (named CANYON-B and CONTENT; Bittig et al., 2018) are now also used to help inform decisions regarding GLODAP data quality control or to fill in observational gaps (Olsen et al., 2019, 2020; Tanhua et al., 2019, 2021). The GLODAP data products have also been successfully used to construct new Global Ocean A_T and C_T climatological monthly fields at the surface and in the water

column using neural network methods (e.g., Broullón et al., 2019, 2020).

Following pioneer works that produced various global-ocean climatologies of the sea-surface carbonate system (Millero et al., 1998; Lee et al., 2000, 2006; Takahashi et al., 2002, 2009, 2014; Sasse et al., 2013; Jiang et al., 2019), the coupling of fCO_2 data (from SOCAT) and A_T data (from GLODAP) now enables reconstruction of the full carbonate system in the surface ocean at a monthly timescale to investigate temporal trends at a decadal timescale (e.g., Gregor and Gruber, 2021; Keppler et al., 2023).

International projects such as SOCAT and GLODAP offer an important way to synthesize ocean carbon data. In these projects, each observation is quality controlled, offering users high-quality observations for regional or global analysis, either for process analysis or to constrain or validate ocean and coupled climate–carbon models (Coupled Model Intercomparison Project Phase 6 – CMIP6, e.g., Lerner et al., 2021). SOCAT is a publicly available synthesis product initiated in 2007 (Metzl et al., 2007) for quality-controlled surface-ocean fCO_2 observations made by the international marine carbon research community (Bakker et al., 2016). The first SOCAT version was released in 2011 (Pfeil et al., 2013; Sabine et al., 2013), followed by six SOCAT versions (Bakker et al., 2014, 2016). The last version in 2023 included more than 40 million fCO_2 data with an accuracy better than 5 µatm (Bakker et al., 2023). One important component of SOCAT is the use of data to estimate global air–sea CO_2 fluxes based on reconstructed pCO_2 fields (e.g., Surface Ocean pCO_2 Mapping Intercomparison – SOCOM; Rödenbeck et al., 2015). Since 2015, these results have been included in the estimate of the global carbon budget each year (Le Quéré et al., 2015; Friedlingstein et al., 2022).

On the other hand, following the World Ocean Circulation Experiment (WOCE) and Joint Global Ocean Flux Study (JGOFS) era in the 1990s, when almost all observations were started to be synthesized in a specific recommended format (Joyce and Corry, 1994), GLODAP focused on water-column carbon observations (and other properties). Following the original GLODAP data product (Key et al., 2004), the project accumulated many new quality-controlled observations. One important achievement of GLODAP has been the use of data to estimate the anthropogenic CO_2 inventory or its change over decades (Sabine et al., 2004; Gruber et al., 2019). Both products, SOCAT and GLODAP, are relevant tools to detect oceanic acidification rates (Lauvset et al., 2015; Jiang et al., 2019; Feely et al., 2023; Ma et al., 2023).

Although these projects include many international ocean observations, there are ocean-CO_2-related observations all around the world (published or unpublished), such as total alkalinity and dissolved inorganic carbon, that are not included in SOCAT nor GLODAP. This is because SOCAT accepts and controls only fCO_2 data, whereas GLODAP includes and controls water-column data, mainly from WOCE, Global Ocean Ship-based Hydrographic Investigations Program (GO-SHIP), and Climate Variability and Predictability Experiment (CLIVAR) cruises. It should be noted that many ocean carbon observations in various formats can be also found in dedicated database, such as the National Centers for Environmental Information (NCEI) Ocean Carbon and Acidification Data System (OCADS) (formerly CDIAC-Ocean; Jiang et al., 2023b, https://www.ncei.noaa.gov/products/ocean-carbon-acidification-data-system, last access: 22 December 2023), PANGAEA (https://www.pangaea.de/, last access: 22 December 2023) or SEANOE (https://www.seanoe.org/, last access: 22 December 2023). In this context, progress in the data synthesis of ocean carbon observations that would offer new high-quality products for the community (e.g., for GOA-ON, http://www.goa-on.org, last access: 22 December 2023, IOC/SDG 14.1.3, https://oa.iode.org/, last access: 22 December 2023, Tilbrook et al., 2019) is recommended.

In this work, we present a synthesis of more than 44 400 A_T and C_T observations obtained over the 1993–2022 period during various cruises or at time series' stations mainly supported by French projects. This dataset merges observations measured with the same instruments and is, thus, analytically coherent. Most of the data have an accuracy better than $\pm 4\,\mu mol\,kg^{-1}$, i.e., between the climate ($\pm 2\,\mu mol\,kg^{-1}$) and weather ($\pm 10\,\mu mol\,kg^{-1}$) goals (Newton et al., 2015; Bockmon and Dickson, 2015). Hereafter, this dataset will be referred to as SNAPO-CO2-v1. We describe the data assemblage and associated quality control and discuss some potential uses of this dataset.

2 Data collection

The time series' projects and research cruises during which data were collated are listed in Table 1, with the corresponding references given in the Supplement (Table S1) and the sampling locations displayed in Fig. 1. Sampling was performed either from CTD-rosette casts (Niskin bottles) or from the ship's seawater supply (intake at about 5 m depth, depending on the ship and swell). Samples collected in 500 mL borosilicate glass bottles were poisoned with 100–300 µL of $HgCl_2$ (depending on the cruise) and closed with greased stoppers (Apiezon®) that were held tight using an elastic band, following the standard operating procedure (SOP) protocol (Dickson et al., 2007). Some samples were also collected in 500 mL bottles closed with screw caps. After the completion of each cruise, discrete samples were returned back to the LOCEAN (Laboratoire d'Océanographie et du Climat: Expérimentations et Approches Numériques) laboratory (Paris, France) and stored in a dark room at 4 °C before analysis; analysis generally took place within 2–3 months of sampling (sometimes within a week). Some samples were also measured for specific process studies on benthic corals (e.g., Maier et al., 2012; McCulloch et al., 2012) or for mesocosm and culture experiments, but these data are

not included in this synthesis because they do not represent the natural ocean state (e.g., the addition of Sahara dust during the "DUst experiment in a low-Nutrient, low-chlorophyll Ecosystem" project – DUNE; Ridame et al., 2014).

As opposed to pCO_2, surface A_T or C_T observations are generally obtained from discrete sampling (measured aboard a vessel or onshore). Few cruises offer semicontinuous sea-surface A_T or C_T observations (e.g., Metzl et al., 2006), but new instrumental developments (Seelmann et al., 2020) have now enabled A_T measurements on Ship of Opportunity Program (SOOP) lines. In addition to discrete samples analyzed for various projects conducted mainly in the North Atlantic, tropical Atlantic, tropical Pacific, Mediterranean Sea and coastal regions (Table 1), we complemented this synthesis with A_T and C_T surface observations obtained in the Indian and Southern oceans during the OISO (Océan Indien Service d'Observation) cruises in 1998–2018 (Metzl et al., 2006; Leseurre et al., 2022; data also available from NCEI OCADS: https://www.nodc.noaa.gov/ocads/oceans/VOS_Program/, last access: 22 December 2023) and the recent CLIM-EPARSES cruise conducted in the Mozambique Channel in April 2019 (Lo Monaco et al., 2020, 2021). For OISO cruises, the water-column observations are part of the CARINA (CARbon IN the Atlantic) and GLODAP synthesis products (Lo Monaco et al., 2010; Olsen et al., 2016, 2019, 2020) and are not included here. Except when otherwise specified, all data in this synthesis were obtained using the same technique used in either the laboratory or at sea (for the OISO 1998–2018 and CLIM-EPARSES 2019 cruises).

3 Method, accuracy, repeatability, intercomparison and quality control

3.1 Method and accuracy

Since 2003, the discrete samples returned to the SNAPO-CO2 service facilities (LOCEAN, Paris) have been simultaneously analyzed for A_T and C_T using potentiometric titration with a closed cell (Edmond, 1970; Goyet et al., 1991). The same technique was used at sea for underway surface water measurements during OISO and CLIM-EPARSES cruises (indicated using the footnote in Table 1). For two time series, the dataset also includes measurements obtained before 2000 using other techniques: the DYFAMED time series' observations measured between 1998 and 2000 in the Mediterranean Sea (Copin-Montégut and Bégovic, 2002; Coppola et al., 2020) and the SURATLANT time series' values acquired from 1993 to 1997 in the North Atlantic subpolar gyre (Reverdin et al., 2018). We also include A_T data from the river La Penzé (Brittany) from 2019 to 2020 (Yann Bozec, Station Biologique de Roscoff – SBR, personal communication, 2020).

In the late 1980s, the so-called "JGOFS-IOC Advisory Panel on Ocean CO_2" highlighted the need for standard analysis protocols and for the development of Certified Reference Materials (CRMs) for inorganic carbon measurements (Poisson et al., 1990; UNESCO, 1990, 1991). The CRMs were provided to international laboratories by Andrew Dickson (Scripps Institution of Oceanography, San Diego, USA), starting in 1990 for C_T and in 1996 for A_T. Thus, these CRMs were available during this work and were used to calibrate the measurements (CRM batch numbers used for each cruise are listed in Table S2 in the Supplement). The concentrations of the CRMs that we used varied between 2193 and 2426 µmol kg^{-1} for A_T and between 1968 and 2115 µmol kg^{-1} for C_T, corresponding to the range of concentrations observed in open-ocean water. The CRM accuracy, as indicated on the certificate for each batch, is around ±0.5 µmol kg^{-1} for both A_T and C_T (https://www.nodc.noaa.gov/ocads/oceans/Dickson_CRM/batches.html, last access: 22 December 2023).

The results of analyses performed on 965 CRM bottles (different batches) between 2013 and 2023 are presented in Fig. 2. The standard deviations of the differences in measurements were around ±3.5 µmol kg^{-1} on average for both A_T and C_T. For unknown reasons, the differences were occasionally up to 10–15 µmol kg^{-1} (0.8 % of the data; Fig. S2). These few CRM measurements were discarded with respect to the data processing. On average, excluding some outliers, standard deviations of the differences for 1090 CRM analyses were ±2.71 µmol kg^{-1} for A_T and ±2.86 µmol kg^{-1} for C_T. We did not detect any specific signal for CRM analyses (e.g., larger uncertainty depending on the batch number or temporal drifts during analyses; Fig. 2); however, for some cruises, the accuracy based on CRMs could be slightly better than 3 µmol kg^{-1} (e.g., Marrec et al., 2014; Touratier et al., 2016; Ganachaud et al., 2017; Wimart-Rousseau et al., 2020).

3.2 Repeatability

For some projects, duplicates have regularly been sampled (e.g., SOMLIT-Point-B, SOMLIT-BREST and BOUSSOLE/DYFAMED) or replicate bottles have been sampled at selected depths at fixed stations during the cruises (e.g., OUTPACE 2015 and SOMBA 2014). The results of A_T and C_T repeatability are synthesized in Table 2. Figure 3 shows an example of regular duplicates from the following times series: SOMLIT-Point-B in the coastal Mediterranean Sea, SOMLIT-BREST in the Bay of Brest in the coastal Iroise Sea and BOUSSOLE/DYFAMED in the Ligurian Sea. For the 26 OISO cruises conducted between 1998 and 2018 and the CLIM-EPARSES cruise in April 2019, the repeatability was evaluated from duplicate analyses (within 20 min) of continuous underway sea-surface samples at the same location (when the ship was stopped). Similarly to what was found for the CRM measurements (Fig. S2), differences in duplicates are occasionally higher than 10–15 µmol kg^{-1} (Fig. 3), although most of the duplicates for all projects are

Table 1. List of cruises in the SNAPO-CO2-v1 dataset. This is organized by region for the Global Ocean and coastal zones and for the Mediterranean Sea (MedSea). The reader is referred to Tables S1, S2, S4 and S4 in the Supplement for a list of the laboratories, the CRMs used, the corresponding references and the DOIs of cruises. Nb denotes the number of data for each cruise or time series.

Cruise/Project	Start	End	Region	Sampling	Nb
AWIPEV	2015	2021	Arctic	Surface and subsurface	195
SURATLANT and RREX	1993	2017	North Atlantic	Surface	2832
OVIDE	2006	2018	North Atlantic	Surface and water column	397
STRASSE	2012		North Atlantic	Water column	205
EUREC4A-OA	2020		North Atlantic	Surface and water column	135
PROTEUS	2010		North Atlantic	Water column	27
CHANNEL	2012	2015	English Channel	Surface	696
SOMLIT-BREST	2008	2019	Coastal North Atlantic	Surface	1174
SOMLIT-Roscoff	2009	2019	Coastal North Atlantic	Surface and 60 m	801
ECOSCOPA	2017	2019	Coastal North Atlantic	Surface	67
Penzé	2011	2020	Brittany, river	Surface and subsurface	148
Aulne	2009	2010	Brittany, river	Surface	27
Élorn	2009	2009	Brittany, river	Surface	28
BIOZAIRE	2003	2004	Tropical Atlantic	Water column	87
EGEE	2005	2007	Tropical Atlantic	Surface	199
PIRATA-FR	2009	2017	Tropical Atlantic	Surface and water column	513
PLUMAND	2007		Tropical Atlantic	Surface	38
OUTPACE	2015		Tropical Pacific	Water column	240
PANDORA	2012		Solomon Sea	Water column	178
Tara Pacific	2016	2018	Tropical Pacific–North Atlantic	Surface and subsurface	325
Tara Ocean	2009	2012	Global Ocean	Surface and 400 m	123
Tara Microbiome	2021	2022	Atlantic	Surface and water column	216
ACE	2016	2017	Southern Ocean	Surface and water column	135
MOBYDICK	2019		Southern Ocean	Water column	64
CLIM-EPARSES*	2019		Indian	Surface	790
OISO*	1998	2018	South Indian	Surface	24 950
DYFAMED	1998	2017	MedSea	Water column	2118
BOUSSOLE	2014	2019	MedSea	Surface and 10m	172
SOMLIT-Point-B	2007	2015	MedSea, coastal	Surface and 50 m	2397
ANTARES	2010	2016	MedSea	Water column	502
MOLA	2010	2013	MedSea, coastal	Water column	66
SOLEMIO	2016	2018	MedSea, coastal	Water column	212
MOOSE-GE	2010	2019	MedSea	Water column	1847
LATEX	2010		MedSea	Water column	51
CARBORHONE	2011	2012	MedSea	Water column	706
CASCADE	2011		MedSea	Water column	218
DEWEX	2013		MedSea	Water column	367
SOMBA	2014	2014	MedSea	Water column	203
AMOR-BFLUX	2015		MedSea, coastal	Water column	6
PEACETIME	2017	2017	MedSea	Water column	233
PERLE	2018	2021	MedSea	Water column	805

* Measurements were taken at sea (surface measurement while underway).

within 0–3 µmol kg^{-1}. Based on the CRM analyses and replicates for different projects, different regions and different periods, we estimated A_T and C_T data to be consistent with an accuracy of better than 4 µmol kg^{-1}.

3.3 Intercomparisons

Intercomparisons of measurements performed with different techniques help to evaluate the quality of the data and detect potential biases when merging different laboratories' data obtained from the same region during different periods. This is especially important to interpret long-term trends in A_T and C_T as well as for pCO_2 and pH calculated with A_T–C_T pairs. For ocean acidification studies, this also refers to the

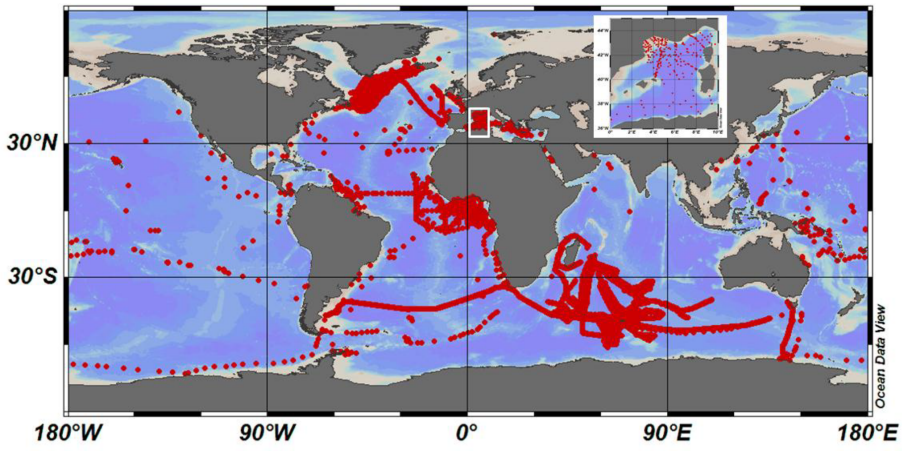

Figure 1. Locations of A_T and C_T data (1993–2022) in the Global Ocean and the western Mediterranean Sea (white box, inset) in the SNAPO-CO2-v1 dataset. The figure was produced with Ocean Data View (ODV; Schlitzer, 2018).

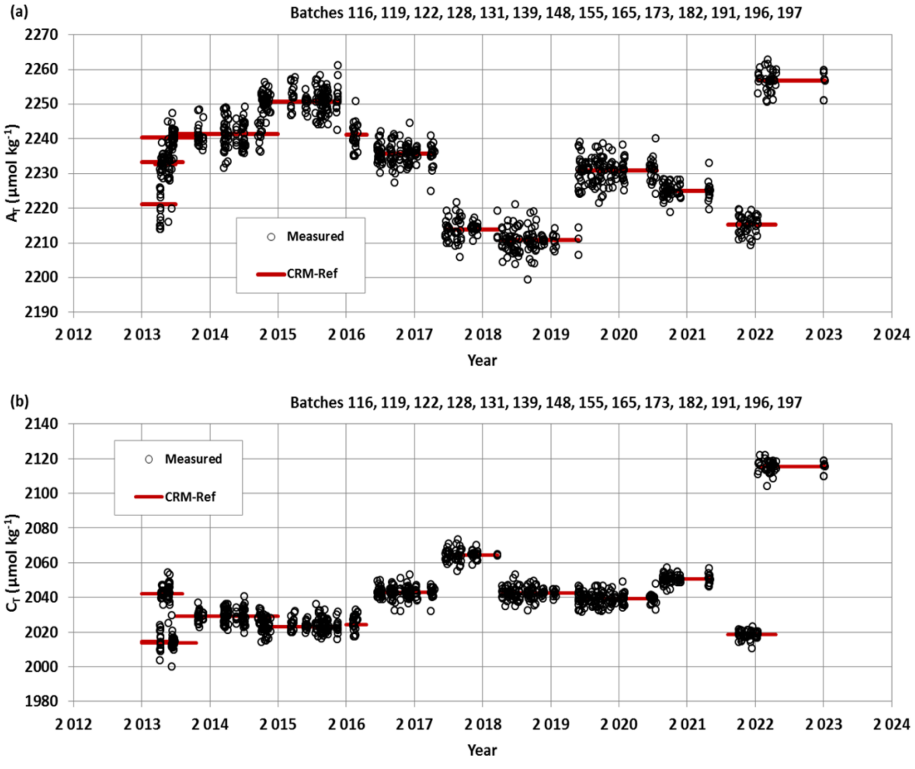

Figure 2. A_T **(a)** and C_T **(b)** analyses for different CRM batches measured in the 2013–2023 period. For these 965 analyses, the means (standard deviations) of the differences with the CRM reference were −0.1 (±3.4) µmol kg^{-1} for A_T and 0.1 (±3.7) µmol kg^{-1} for C_T.

"climate goal", for which an accuracy for A_T and C_T of better than ±2 µmol kg^{-1} is needed (Newton et al., 2015; Tilbrook et al., 2019). For the projects in this data synthesis, inter-laboratory comparisons were occasionally performed and are summarized below.

3.3.1 CHANNEL project

As part of the CHANNEL (2012–2015) time series in the western English Channel, Marrec et al. (2014) analyzed surface samples collected bimonthly from 2011 to 2013. A_T analyses were performed with a TA-ALK-2 system (Apollo SciTech), while C_T measurements were acquired with an AIRICA (Automated Infra Red Inorganic Carbon Analyzer) system (Marianda Inc.) Based on CRM analyses (batch

Table 2. Repeatability of the A_T and C_T analyses for cruises with duplicate analysis. The results are expressed as the standard deviation (SD) values of the analysis of replicated samples. Nb denotes the number of replicates for each time series or cruise (see Fig. 3 for the results of regular duplicates for three time series: SOMLIT-Point-B, SOMLIT-BREST and BOUSSOLE). For the 26 OISO cruises (1998–2018) and for simplicity, we list the mean repeatability obtained for all cruises.

Cruise	Nb	SD A_T ($\mu mol\,kg^{-1}$)	SD C_T ($\mu mol\,kg^{-1}$)	Reference
OUTPACE	12	3.64	3.68	Wagener et al. (2018a)
SOMBA	13	2.00	3.30	Keraghel et al. (2020)
SOMLIT-Point-B	786	2.63	3.10	Kapsenberg et al. (2017)
SOMLIT-BREST	446	3.34	3.67	Salt et al. (2016) and unpublished information
BOUSSOLE	48	3.47	4.02	Merlivat et al. (2018) and Golbol et al. (2020)
CLIM-EPARSES	122	2.20	2.30	Lo Monaco et al. (2020, 2021)
OISO 1998–2018	1162	2.06	2.28	Metzl et al. (2006) and OISO Lines information[a]

[a] Metadata and data available at https://www.nodc.noaa.gov/ocads/oceans/VOS_Program/OISO.html (last access: 22 December 2023).

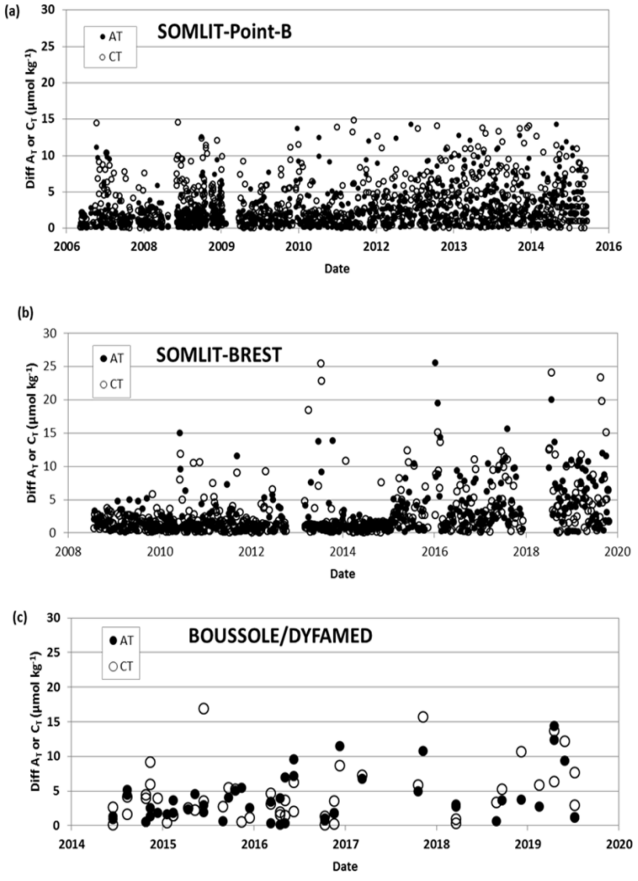

Figure 3. Results of duplicate A_T and C_T analyses from the following time series: **(a)** SOMLIT-Point-B in the coastal Mediterranean Sea (Kapsenberg et al., 2017), **(b)** SOMLIT-BREST in the Bay of Brest in the coastal Iroise Sea (Salt et al., 2016, and unpublished information) and **(c)** BOUSSOLE/DYFAMED in the Ligurian Sea (Merlivat et al., 2018; Golbol et al., 2020). The plots show differences in duplicates for both A_T (filled circles) and C_T (open circles). SD values of these duplicates are listed in Table 2.

no. 92), the accuracy was estimated to be $\pm 3\,\mu mol\,kg^{-1}$ for A_T and $\pm 1.5\,\mu mol\,kg^{-1}$ for C_T (Marrec et al., 2014). When undertaking a comparison with the samples measured at LOCEAN, Paris, for the year 2012, Marrec et al. (2014) concluded that the concentrations between the two methods were within ± 2 and $\pm 3\,\mu mol\,kg^{-1}$ for A_T and C_T, respectively. This is close to the aforementioned climate goal, offering confident results for long-term trend analysis of the carbonate system in this region.

3.3.2 SURATLANT project

In the framework of the SURATLANT project in the subpolar North Atlantic gyre, some samples collected at the same time (in 2005, 2006, 2010, 2015 and 2016) were also analyzed onshore for A_T and/or C_T by other laboratories using different techniques (e.g., coulometric method); these results have been summarized by Reverdin et al. (2018). For C_T, the mean (SD) differences between LOCEAN values and those from four other laboratories range between -0.7 (± 4.6) and -6.5 (± 3.4) $\mu mol\,kg^{-1}$, depending on the cruise. For A_T, the mean differences compared with two other laboratories range from -0.6 (± 4.1) $\mu mol\,kg^{-1}$ to $+2.3$ (± 4.8) $\mu mol\,kg^{-1}$.

3.3.3 OVIDE project

During OVIDE cruises, which have been conducted since 2002 in the North Atlantic along a section from Greenland to Portugal (Lherminier et al., 2007; Mercier et al., 2015), samples have been taken (since 2006) to complement (for summer) the SURATLANT time series in the North Atlantic subpolar gyre (NASPG). The OVIDE samples at the surface and along the water column at a few stations were measured back at LOCEAN for A_T and C_T (Metzl et al., 2018). This enabled us to compare our data with the onboard measurements performed by the IIM (Instituto de Investigaciones Marinas) group in Vigo, Spain (e.g., Pérez et al., 2010, 2013, 2018; Vazquez-Rodriguez et al., 2012). The OVIDE data

have been regularly quality controlled as part of the CARINA and GLODAP data products (Velo et al., 2009; Key et al., 2010; Olsen et al., 2016, 2019, 2020). The results of intercomparisons are gathered in Table 3. For OVIDE in 2006, we identified (for unknown reason) a large difference between our original A_T values and the A_T data qualified in GLODAP; thus, we corrected our A_T data by $+7.2\,\mu mol\,kg^{-1}$. However, no correction was applied to C_T data. For other OVIDE cruises, differences in A_T values range between -4.5 (± 4.11) $\mu mol\,kg^{-1}$ and -0.05 (± 3.43) $\mu mol\,kg^{-1}$, depending on the cruise (i.e., A_T measured at LOCEAN was always slightly lower than onboard measurements). For C_T, we compared our onshore measurements with C_T values calculated with A_T and pH measured on board. Most of the mean C_T differences are slightly positive (i.e., C_T measured at LOCEAN was always higher, except for 2010). Considering all errors associated with sampling, the transport of samples, the instrumentation, the data processing or the calculation of C_T using A_T–pH pairs (around $8.8\,\mu mol\,kg^{-1}$; Orr et al., 2018), the comparisons between LOCEAN and IIM data for OVIDE cruises are deemed acceptable, and large differences in both A_T and C_T ($>4\,\mu mol\,kg^{-1}$) are far from being systematic (Table 3). The data from SURATLANT and OVIDE can then be merged to complete the time series in the NASPG in summer and to better describe the seasonality of the oceanic carbonate system. For example, in 2010, when the North Atlantic Oscillation (NAO) was strongly negative, the SURATLANT data showed a rapid decrease in C_T concentrations in the NASPG between early-June and August (Fig. 4), with C_T concentrations in August being much lower than other years (Racapé et al., 2014). This led to a rapid drop in fCO_2 in 2009–2010, such that the NASPG was a strong CO_2 sink (Leseurre et al., 2020). The winter-to-summer seasonal decrease in C_T in 2010 in the northern NASPG was on average $-77\,\mu mol\,kg^{-1}$ (Fig. 4), much larger than in the climatology (range of -50 to $-55\,\mu mol\,kg^{-1}$; Takahashi et al., 2014; Reverdin et al., 2018). The OVIDE data in late June in 2010 and SURATLANT in August 2010 confirmed this signal that was linked to pronounced primary productivity in that period (Fig. 4; Henson et al., 2013; Racapé et al., 2014; McKinley et al., 2018). Note that, for this period, no fCO_2 observations were available in July–September 2010 in the SOCAT data product and that the A_T and C_T data presented here could be used to calculate fCO_2 to complement the fCO_2 dataset in this region, as was done for other periods (McKinley et al., 2011).

3.3.4 The river La Penzé

The comparisons described above concern the open-ocean region that has A_T and C_T concentrations in a range of concentrations close to the CRM references (used by the different laboratories). Another example of a comparison is presented here for samples obtained along a river and, thus, for waters with a low salinity and low A_T concentrations (river La Penzé in northern Brittany). In 2019–2020, A_T was measured at SBR laboratory using a potentiometric method (with a Titrino 847 plus Metrohm) calibrated with CRM (batch no. 131) for a final accuracy of $\pm 2.1\,\mu mol\,kg^{-1}$ (Gac et al., 2020). Although the samples were measured with different techniques, the A_T–salinity relationships are very coherent for both datasets (Fig. 5). The regressions for each period for A_T (in $\mu mol\,kg^{-1}$) are as follows:

- $A_T = 51.525\ (\pm 0.944)\ S + 583.95\ (\pm 19.94)$ ($r^2 = 0.975$) (for 78 samples in 2011);
- $A_T = 54.022\ (\pm 1.018)\ S + 450.23\ (\pm 31.53)$ ($r^2 = 0.976$) (for 70 samples in 2019–2020).

Therefore, we added the A_T data measured in 2019–2020 to complete the synthesis for this location (river La Penzé).

3.4 Assigned flags for quality control

Identifying each data point with an appropriate flag is very convenient for selecting data (good, questionable or bad data). Here, following the WOCE program, we used four flags for each property (Flag 2 – good data, Flag 3 – questionable data, Flag 4 – bad data and Flag 9 – no data), as used in other data products such as SOCAT (Bakker et al., 2016) or GLODAP (Olsen et al., 2016, 2019, 2020; Lauvset et al., 2021). During data processing, we first assigned a flag for each A_T and C_T data point based on the standard error in the calculation of A_T and C_T concentrations (nonlinear regression; Dickson et al., 2007). By default, if the standard deviation of the regression was $>1\,\mu mol\,kg^{-1}$, we assigned Flag 3 (questionable), although the data could be acceptable and then used for interpretations. Flag 3 was also assigned when salinity was doubtful or when differences between duplicates were large (e.g., $\pm 20\,\mu mol\,kg^{-1}$). Flag 4 (bad or certainly bad) was assigned when clear anomalies were detected for unknown reasons (e.g., a sample probably not fixed with $HgCl_2$). A secondary quality control was performed by the principal investigator of each project based on data inspection, duplicates, the A_T–salinity relationship, or the mean observations in deep layers where large variability in A_T and C_T is unlikely to occur from year to year. An example presents all data from the MOOSE-GE cruises conducted in 2010–2019 in the Mediterranean Sea (Coppola et al., 2020; Testor et al., 2010) where clear outliers have been identified (Fig. S3). For the 10 MOOSE-GE cruises and a total of 1847 A_T and C_T analyses, 26 data points were flagged as bad (Flag 4), 139 data points for A_T and 141 data points for C_T were listed as questionable (Flag 3), and 1682 data points for A_T and 1680 data points for C_T were considered to be good data (Flag 2, i.e., more than 90 %). A similar control process was performed for each project.

The synthesis of various cruises in the same region and period also offers verification and secondary control of the data. For example, several cruises were conducted in the Mediterranean Sea in 2014 (MOOSE-GE, SOMBA, ANTARES and

Table 3. Comparisons of A_T and C_T samples measured back at LOCEAN with onboard measurements by IIM laboratory (Fiz Pérez, Vigo, Spain) for OVIDE cruises in the North Atlantic. Nb denotes the number of samples and ND denotes no data. The results listed indicate the means and standard deviations of the differences (LOCEAN – IIM). For A_T, IIM values were measured on board. For C_T, IIM values were calculated from A_T and pH, both measured on board. Here, the IIM data were quality controlled and taken from the GLODAP data products (Olsen et al., 2016, 2019).

Cruise and year	Nb A_T	A_T (LOCEAN) – A_T (IIM) µmol kg^{-1}	Nb C_T	C_T (LOCEAN) – C_T (IIM) µmol kg^{-1}
OVIDE 2006	14	−2.0 (±5.9)*	14	1.1 (±2.5)
OVIDE 2008	29	−4.5 (±4.1)	29	3.8 (±3.1)
OVIDE 2010	41	−2.0 (±2.3)	41	−2.4 (±3.3)
OVIDE 2012	37	−0.1 (±8.8)	ND	ND
GEOVIDE 2014	57	-0.1 (±3.4)	54	2.4 (±7.9)

* For the OVIDE 2006 cruise, the original difference in A_T was −9.0 (±5.8) µmol kg^{-1}. LOCEAN A_T data were corrected by +7.2 µmol kg^{-1} based on the mean concentrations in deep layers, whereas no corrections were applied for A_T and C_T for other cruises.

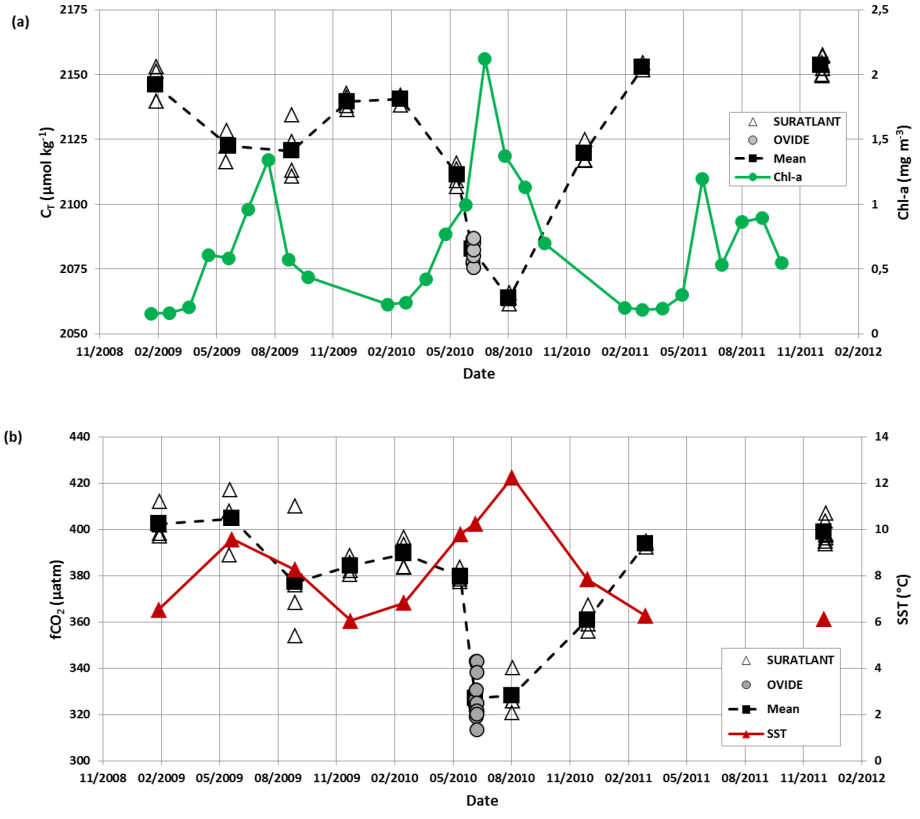

Figure 4. **(a)** Time series of C_T concentrations (µmol kg^{-1}) for 2009–2011 in surface waters in the North Atlantic subpolar gyre (zone 59° N, 33° W) based on SURATLANT (open triangles) and OVIDE 2010 (gray circles) data. In 2009, SURATLANT data were available in February, June, September and December; in 2010, data were available in March, June, August and December; and in 2011, data were only available for March and December. The OVIDE data in late June in 2010 completed the temporal cycle and confirmed the strong seasonal signal and low C_T concentrations in summer 2010 not seen in 2009 (nor in 2011, as there were no data in summer). The mean observations for each period describe the C_T seasonal cycles in 2009 and 2010 (black squares, dashed line). The monthly surface chlorophyll-*a* (Chl-*a*) concentrations (mg m^{-3}) averaged in the same region based on MODIS are also shown (green dots and line), highlighting the high productivity during the summer 2010. Chl-*a* monthly data were extracted from MODIS (Giovanni, NASA, last access: 3 May 2019). **(b)** Time series of fCO_2 (µatm) for the same cruises (same symbols) were calculated with A_T and C_T and using the K_1 and K_2 constants from Lueker et al. (2000). The mean sea-surface temperature (SST, °C) is also indicated (red triangles). In June 2010, oceanic fCO_2 decreased by 53 µatm in 2 weeks.

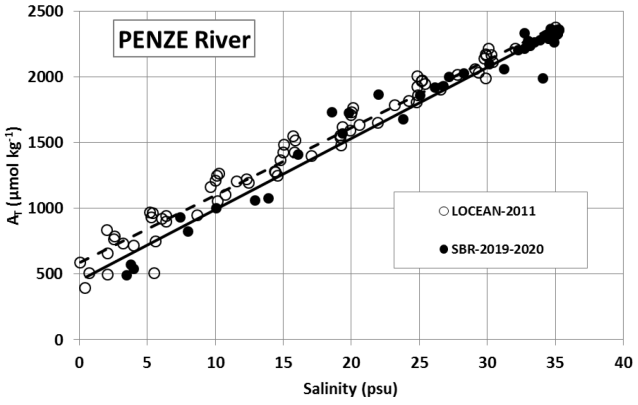

Figure 5. Total alkalinity (A_T) versus salinity for samples measured in 2011 and 2019 in the river La Penzé, northern Brittany (Gac et al., 2020). A_T samples were measured at LOCEAN in 2011 (open circles, dashed line) and at SBR laboratory (Roscoff) in 2019 (filled circles, black line).

DYFAMED). The mean values of C_T and A_T in the deep layers (>1800 m) for each cruise confirmed the coherence of the data (Table 4). This enabled us to merge the different datasets in order to interpret the temporal trends and processes driving the CO_2 cycle (Coppola et al., 2019, 2020) or to train and validate a regional neural network to reconstruct the carbonate system (e.g., CANYON-MED; Fourrier et al., 2020, 2022).

The total number of data for the Global Ocean and the Mediterranean Sea are gathered in Table 5 with the corresponding flags for each property. Overall, the synthesis includes more than 94 % of good data for both A_T and C_T. About 5 % of data are questionable and 2 % are likely bad. Overall, we believe that all data (with Flag 2) in this synthesis have an accuracy of better than 4 µmol kg^{-1} for both A_T and C_T, which is the same as for quality-controlled data in GLODAP (Olsen et al., 2020; Lauvset et al., 2021). The uncertainty ranges between the climate goal (2 µmol kg^{-1}) and the "weather goal" (10 µmol kg^{-1}) for ocean acidification studies (Newton et al., 2015; Tilbrook et al., 2019). This accuracy is also relevant to validate or constrain data-based methods that reconstruct A_T and C_T fields with an error of around 10–15 µmol kg^{-1} for both properties (Bittig et al., 2018; Broullón et al., 2019, 2020; Fourrier et al., 2020).

3.5 Using A_T and C_T to calculate fCO_2 and pH for comparison with fCO_2 and pH measurements

For some projects, the A_T and C_T data presented in this synthesis were used to calibrate or validate in situ fCO_2 sensors (Bozec et al., 2011; Marrec et al., 2014; Merlivat et al., 2018). The A_T and C_T data were also used to calculate fCO_2 and to derive associated air–sea CO_2 fluxes, especially during periods when no direct fCO_2 measurements were available (e.g., in the North Atlantic; Fig. 4; Watson et al., 2009; McKinley et al., 2011). For example, Marrec et al. (2014) successfully used the calculated pCO_2 (with A_T–C_T pairs) to adjust the drift of the pCO_2 data recorded with a CONTROS HydroC CO_2 FT sensor mounted on a FerryBox for regularly sampling the western English Channel (CHANNEL project). Here, we show the results for the 2012–2014 period (Fig. 6). In this region, the total alkalinity is relatively constant over time: the average A_T for 528 samples from different seasons and years is 2334.4 (±7.2) µmol kg^{-1}. Conversely, the C_T concentrations show distinctive seasonality, with higher concentrations in winter and lower concentrations in summer when biological activity is pronounced (Marrec et al., 2013, 2014; Kitidis et al., 2019). This controls the seasonal pCO_2 distribution revealed each year in both the measured and calculated pCO_2 (Fig. 6). For 528 co-located samples, the mean difference between calculated and measured pCO_2 is −1.9 (±11.9) µatm, with no distinct differences depending on the season and year.

In the Ligurian Sea, following the first high-frequency in situ fCO_2 measurements in 1995–1997 at the DYFAMED time series' station (Hood and Merlivat, 2001), a new CARIOCA fCO_2 sensor was deployed at that location in 2013 (BOUSSOLE project; Merlivat et al., 2018). The CARIOCA sensor was calibrated with regular A_T and C_T analyses performed at LOCEAN. Based on these data, the mean difference between CARIOCA fCO_2 measurements and calculated fCO_2 data was estimated to be around ±4.4 µatm for 2013–2015, i.e., of the same order as the precision of the CARIOCA sensor (±5 µatm; Merlivat et al., 2018). Here, we extend the results for the 2013–2018 period (Golbol et al., 2020; data also in SOCAT version v2021 in Bakker et al., 2016) and compared the CARIOCA fCO_2 time series with A_T and C_T data from different cruises (BOUSSOLE, DYFAMED and MOOSE-GE) selected in the 0–20 m layer at that location (Fig. S4). For 67 co-located samples from different seasons and years, the mean difference between calculated and measured fCO_2 ($fCO_{2cal} - fCO_{2mes}$) was −3.7 (±10.8) µatm where fCO_2 was calculated from A_T–C_T pairs using the constant from Lueker et al. (2000). At the location of the BOUSSOLE mooring in the Ligurian Sea (shown in Fig. S4), the alkalinity is relatively constant over the 2013–2018 period, with an average concentration of 2569.8 (±13.2) µmol kg^{-1}. In contrast, C_T concentrations show a clear seasonality, decreasing by around 50 µmol kg^{-1} from winter to late summer, driving the large seasonal cycle of fCO_2 (range 80 µatm) revealed in both measured and calculated values (here, fCO_2 is normalized at 13 °C; Fig. S4). In addition to calibration purposes, a regional A_T–salinity relationship was derived from the A_T data measured at that location and successfully used to construct time series of C_T and pH calculated from the high-frequency CARIOCA fCO_2 data to investigate and interpret the long-term change in fCO_2 and acidification in the Ligurian Sea (Merlivat et al., 2018; Coppola et al., 2020).

Table 4. Mean observations in the deep layers (>1800 m) of the western Mediterranean Sea for different cruises conducted in 2014. Results for deep layers (>1800 m) for the DEWEX cruise in 2013 and the PEACETIME cruise in 2017 in the same region are also listed. N-A_T and N-C_T are A_T and C_T normalized at a salinity of 38, respectively. Nb denotes the number of data (with Flag 2). Standard deviations are shown in parentheses. References for these cruises are listed in the Supplement.

Cruise	Period	Nb	Potential temperature (°C)	Salinity (PSU)*	N-A_T (µmol kg^{-1})	N-C_T (µmol kg^{-1})
All cruises	February–December 2014	76	12.905 (0.007)	38.486 (0.005)	2562.9 (5.3)	2303.7 (4.7)
ANTARES	February–November 2014	14	12.913 (0.004)	38.488 (0.006)	2564.0 (3.8)	2301.9 (3.5)
DYFAMED	March–December 2014	9	12.905 (0.0016)	38.487 (0.004)	2560.1 (5.0)	2304.3 (6.8)
MOOSE-GE	July 2014	21	12.909 (0.004)	38.487 (0.005)	2565.6 (4.6)	2303.5 (4.1)
SOMBA	August–September 2014	32	12.899 (0.005)	38.483 (0.005)	2561.5 (5.6)	2304.6 (4.8)
DEWEX	February–April 2013	44	12.903 (0.010)	38.588 (0.006)	2556.0 (4.3)	2294.0 (5.7)
PEACETIME	May–June 2017	7	12.904 (0.002)	38.486 (0.003)	2567.2 (10.6)	2308.1 (8.9)

* PSU represents practical salinity units.

Table 5. Number of temperature, salinity, A_T and C_T data in the synthesis identified for flags 2, 3, 4 and 9. The data are given for the full Global Ocean and for the Mediterranean Sea dataset. The last column is the percentage of Flag 2 (good).

	Flag 2	Flag 3	Flag 4	Flag 9	% Flag 2
Global Ocean					
Temperature	43 538	410	0	478	99.07
Salinity	44 033	319	2	71	99.28
A_T	39 331	2144	1165	1787	92.24
C_T	39 921	2091	1148	1279	92.50
Mediterranean Sea					
Temperature	9843	1	0	65	99.99
Salinity	9879	8	2	20	99.99
A_T	8853	425	411	220	91.37
C_T	8854	451	389	211	91.33

A CARIOCA sensor was also deployed in 2003 near the SOMLIT-BREST time series' site in the Bay of Brest (Bozec et al., 2011; Salt et al., 2016). As for BOUSSOLE in the Ligurian Sea, samples collected for A_T and C_T were used for validation of the pCO_2 recorded by the CARIOCA sensor, and the comparison with calculated pCO_2 showed good agreement, i.e., $pCO_{2cal} = 0.98 \times pCO_{2mes} + 7$ µatm (Bozec et al., 2011). CARIOCA sensors were also deployed on moorings in the tropical Atlantic (PIRATA project; e.g., Lefèvre et al., 2008, 2016; Parard et al., 2010). With the discrete A_T and C_T data included in this synthesis (EGEE and PIRATA-FR cruises), the fCO_2 data from the CARIOCA sensor associated with an adapted A_T–salinity relationship were used to derive pH (Lefèvre et al., 2016) or C_T time series to evaluate net community production in the eastern tropical Atlantic (Parard et al., 2010; Lefèvre and Merlivat, 2012).

Although this is not a direct instrumental intercomparison, differences between pCO_2 (or fCO_2) calculated using A_T–C_T pairs with direct pCO_2 measurements provide a glimpse into the quality of A_T and C_T data in this synthesis, given the uncertainty attached to the pCO_2 or pH calculations (Orr

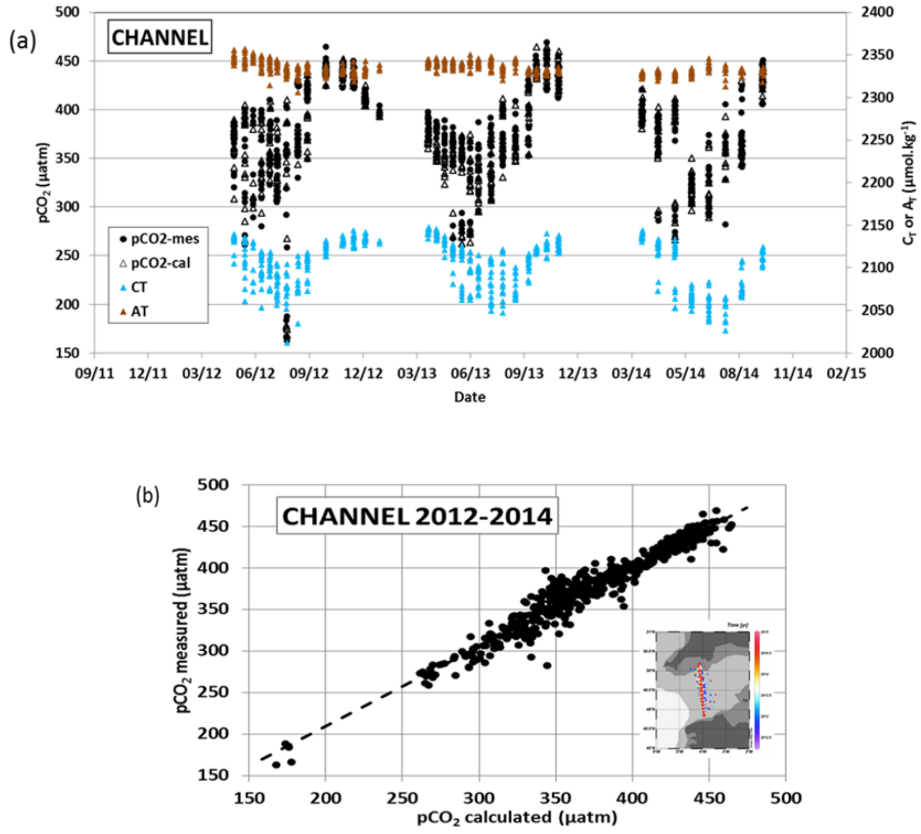

Figure 6. Panel **(a)** presents time series of A_T (brown triangles, right y axis), C_T (blue triangles, right y axis), calculated pCO_2 (open triangles, left y axis) and measured pCO_2 (filled circles) in the western English Channel in 2012–2014 (Marrec et al., 2014). Panel **(b)** shows measured pCO_2 versus calculated pCO_2 for the same samples. The mean difference ($pCO_{2cal} - pCO_{2mes}$) for 528 samples is -1.9 (± 11.9) µatm. Data are from Marrec and Bozec (2016a, b, 2017). Localization of the samples is shown in the inset map in panel **(b)**, which was produced with ODV (Schlitzer, 2018).

et al., 2015). For example, in the framework of the SURATLANT project in the North Atlantic, calculated fCO_2 data were compared with co-located fCO_2 measurements for different seasons and years (Fig. S5). The mean differences ($fCO_{2cal} - fCO_{2mes}$) ranged between -4.3 (± 12.9) µatm (2004–2007, 74 co-located samples) and -3.0 (± 12.1) µatm (2014–2015, 98 co-located samples). The differences are almost the same for different years (and seasons) and are, thus, attributed to method uncertainties (including sampling time, measurement errors and data processing). Based on these comparisons and the consistency between data, we are confident that the A_T and C_T data presented in this synthesis could be used to calculate fCO_2 (and pH) and to interpret temporal changes and drivers of these parameters as well as to estimate air–sea CO_2 fluxes in the North Atlantic (e.g., Corbière et al., 2007; Schuster et al., 2009, 2013; Watson et al., 2009; Metzl et al., 2010; McKinley et al., 2011; Reverdin et al., 2018; Kitidis et al., 2019; Leseurre et al., 2020).

The A_T and C_T data in this synthesis have also been successfully used for fCO_2 and air–sea CO_2 flux calculations in other regions: the tropical Atlantic (Koffi et al., 2010), the tropical Pacific (Moutin et al., 2018; Wagener et al., 2018a), the Solomon Sea (Ganachaud et al., 2017), or the Mediterranean Sea and coastal zones (De Carlo et al., 2013; Marrec et al., 2015; Kapsenberg et al., 2017; Coppola et al., 2020; Keraghel et al., 2020; Wimart-Rousseau et al., 2020; Gattuso et al., 2023).

In addition, A_T and C_T data at the surface and in the water column are also relevant to calculate pH and evaluate its rate of change in the context of addressing the topic of ocean acidification in different regions (Kapsenberg et al., 2017; Ganachaud et al., 2017; Wagener et al., 2018a; Coppola et al., 2020; Leseurre et al., 2020; Lo Monaco et al., 2021). At the ECOSCOPA time series' station in the Bay of Brest (Fleury et al., 2023; Petton et al., 2023), pH values calculated with A_T and C_T data were compared with direct pH measurements (Fig. S6). In 2017–2019, pH (at a standard temperature of 25 °C, hereafter pH-25C) was always lower than 8 and presented a large seasonal signal of 0.3 (high pH values in spring but low values in winter). The mean difference between calculated and measured pH-25C for 46 samples was equal to $+0.013$ (± 0.010), which is in the range of the pH uncertainty

evaluated by error propagation when calculated from A_T–C_T pairs (an A_T and C_T error of $\pm 3\,\mu mol\,kg^{-1}$ leads to a pH error of ± 0.0144). Part of these A_T and C_T data used to calculate pH also helped to interpret the response of marine species to acidification, e.g., pteropodes or coccolithophores (*Emiliania huxleyi*), in the Mediterranean Sea (Howes et al., 2015, 2017; Meier et al., 2014) or in the Southern Ocean (Beaufort et al., 2011). The A_T and C_T data also supported environmental analysis in coral reef ecosystems in the tropical Pacific (Tara expedition; Douville et al., 2022; Lombard et al., 2023; Canesi et al., 2023).

4 Global distribution and relationships from A_T and C_T based on the SNAPO-CO2 dataset

The surface distribution in the Global Ocean based on the SNAPO-CO2 dataset is presented in Fig. 7 for A_T and C_T. In the open ocean, high A_T concentrations are identified in the subtropics in all basins (Jiang et al., 2014; Takahashi et al., 2014), with the highest concentrations of up to $2484\,\mu mol\,kg^{-1}$ found in the central North Atlantic (STRASSE cruise in August 2012; 26° N, 36° W). At the surface and at depth, the A_T–salinity and A_T–C_T relationships are clearly identified and structured at the regional scale (Fig. 8).

In the eastern tropical Atlantic (ETA), where the Congo River impacts the salinity field (Vangriesheim et al., 2009), A_T concentrations range between 2100 and $2400\,\mu mol\,kg^{-1}$. The regional A_T–salinity relationship in the ETA based on data from the EGEE cruises in 2005–2007 (Koffi et al., 2010) is robust and has been validated with more recent measurements from PIRATA-FR cruises in 2010–2019 (Lefèvre et al., 2021). The strong A_T–salinity relationship in the ETA was also recognized using data from the Tara Microbiome cruise in May–July 2022 (Fig. S7). Low salinity (<30) and low A_T (1700–$2200\,\mu mol\,kg^{-1}$) are also observed in the western tropical Atlantic near the Amazon River plume. The A_T–salinity relationships in both river plume regions are very similar (Fig. S7).

For C_T, the lowest concentrations were observed in the coastal regions of the tropical Atlantic, on the eastern side of the Gulf of Guinea ($C_T = 1390\,\mu mol\,kg^{-1}$, BIOZAIRE cruise in 2003; 6° S, 11° E; Vangriesheim et al., 2009) and on the western side of the Gulf of Guinea in the coastal zone off French Guyana ($C_T = 1512\,\mu mol\,kg^{-1}$, PLUMAND cruise in 2007; 5° N, 51° W; Lefèvre et al., 2010). Such low C_T concentrations were also observed in the Amazon River plume (around 5° N, 51° W) during the recent EUREC4A-OA cruise in 2020 and the Tara Microbiome cruise in 2021 ($C_T = 1451\,\mu mol\,kg^{-1}$) leading to low oceanic fCO_2 (<350 µatm) and a CO_2 sink in this region (Olivier et al., 2022).

The high C_T concentrations were mainly observed in the Southern Ocean (OISO and Antarctic Circumpolar Expedition, ACE, cruises), south of the polar front around 50° S, linked to the upwelling of C_T-rich deep water (Fig. 7, Metzl et al., 2006; Wu et al., 2019; Chen et al., 2022). This leads to a high C_T/A_T ratio and a high Revelle factor in the Southern Ocean (Fig. 9; Fassbender et al., 2017). The high C_T content and low temperature in the Southern Ocean also lead to a low calcite and aragonite saturation state (Ω) (Takahashi et al., 2014; Jiang et al., 2015). We calculate Ω from A_T and C_T data at in situ temperature, salinity and pressure. At present, the surface ocean is not undersaturated with regard to aragonite (Fig. 10); however, undersaturation levels ($\Omega\text{-Ar} < 1$) were found at around 500 m in the Southern Ocean (ACE cruise in 2017 and MODYDICK cruise in 2018), 1000 m in the tropical Pacific (PANDORA 2012 and OUTPACE 2015 cruises) and 2200 m in the North Atlantic (OVIDE 2012 and 2014 cruises; see also Turk et al., 2017) (Fig. 10). Samples at 400 m from the Tara Oceans cruise in 2009–2012 also indicated aragonite undersaturation in the equatorial Atlantic, equatorial Pacific and off South America (34° S, 73° W; Chile) associated with equatorial or eastern boundary upwelling systems (Feely et al., 2012; Lauvset et al., 2020).

At the surface, $\Omega\text{-Ar} > 3$ is found in the latitudinal band between 45° S and 54° N, whereas $\Omega\text{-Ar} < 3$ below the critical threshold of $\Omega\text{-Ar} = 3.25$ that represents a limit for the distribution of tropical coral reefs (Hoegh-Guldberg et al., 2007) is observed at very few locations in the tropics.

Compared with the open ocean, A_T concentrations are much higher in the Mediterranean Sea (Copin-Montégut, 1993; Schneider et al., 2007; Álvarez et al., 2023), with values up to $2600\,\mu mol\,kg^{-1}$ (Fig. 8). The A_T and C_T data obtained in 1998–2019 show, on average, a clear contrast between the northern and southern regions of the western Mediterranean Sea (Fig. 11a, b), with a higher concentration in the Ligurian Sea and the Gulf of Lion (Gemayel et al., 2015). However, the basin-scale average distribution view smoothed the mesoscale signals recognized in the Mediterranean Sea (e.g., Bosse et al., 2017; Petrenko et al., 2017). In the Gulf of Lion, the synthesis of 11 cruises conducted from May 2010 to June 2011 (CARBORHONE, CASCADE, LATEX, MOLA and MOOSE-GE) highlights the contrasting distributions of A_T and C_T in the coastal zones and offshore (Fig. 11c, d). The averaging of all data for 1998–2019 also smoothed the seasonal signal and the interannual variability described below.

5 Temporal variations in A_T and C_T: examples from the SNAPO-CO2 dataset

Time series' stations, such as BATS, ESTOC and HOT, in the subtropics and stations in the Irminger Sea or in the Iceland Sea are the only way to detect the long-term change in the ocean carbonate system at the surface and in the water column (Bates et al., 2014). These important time series help to

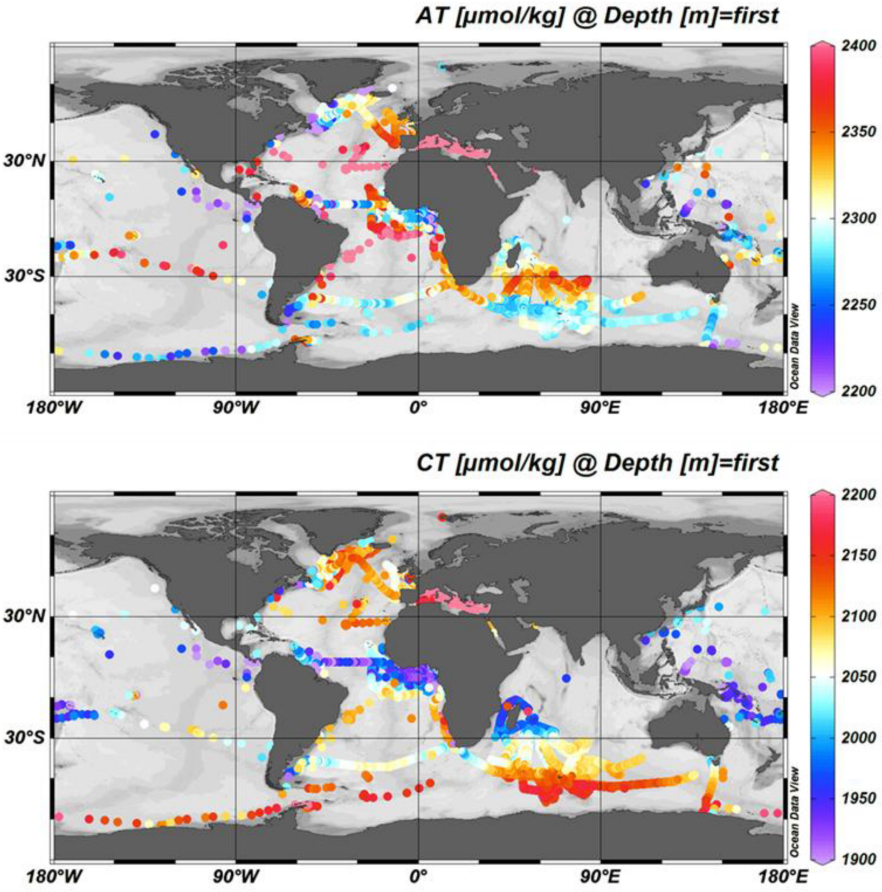

Figure 7. Distribution of A_T (top) and C_T (bottom) concentrations (µmol kg^{-1}) in surface waters (0–10 m). Only data with Flag 2 are presented in these figures. The figure was produced with ODV (Schlitzer, 2018).

understand driving processes (e.g., Hagens and Middelburg, 2016) and are often used to validate the reconstructed pCO_2, A_T, C_T or pH fields (e.g., Rödenbeck et al., 2013; Broullón et al., 2019, 2020; Keppler et al., 2020; Gregor and Gruber, 2021; Ma et al., 2023).

Here, we show examples of the temporal surface variations at locations where data were obtained for more than 10 years (Fig. 12). Thus, we selected the following contrasting regions: the North Atlantic subpolar gyre (NASPG; around 60° N,30° W; 1993–2018 period), the equatorial Atlantic (at 2° N–2° S, 12° W–8° W; 2005–2017 period), the Indian Ocean subtropical sector (26–35° S, 50–56° E; 1998–2018 period), the high-latitude Indian Ocean (54–60° S, 60–70° E; 1998–2018 period), the Ligurian Sea (around DYFAMED station; 43.5–42.5° N, 5.5–9° E; 1998–2019 period) and times series' stations in the coastal zones off Brittany (2008–2019 period).

In the six regions, there was a progressive warming that was most clearly detected in the Mediterranean Sea (e.g., Nykjaer, 2009). From 1998 to 2019, the warming in the Ligurian Sea was +0.1208 °C yr^{-1} (±0.0227 °C yr^{-1}) (Fig. 12). In the equatorial Atlantic, the apparent rapid increase in temperature of +0.48 °C yr^{-1} (±0.04 °C yr^{-1}) in 2005–2017 from the selected data indicated a change in the water masses and circulation. The colder sea surface in 2005 was associated with the so-called Atlantic cold tongue (ACT), which was one of the most intense ACTs since 1982 (Caniaux et al., 2011). The ACT also led to significant changes in oceanic fCO_2 and air–sea CO_2 fluxes (Parard et al., 2010; Koseki et al., 2023) and explained the high C_T concentrations observed in 2005 in this region (Fig. 12, Koffi et al., 2010).

Total alkalinity presents rather homogenous concentrations in the NASPG and the southern Indian Ocean. Interannual variability in A_T is pronounced in the equatorial Atlantic, ranging between 2245 and 2378 µmol kg^{-1}. This is mainly related to salinity, as normalized A_T values (N-A_T, for a salinity of 35) do not show such interannual variability (mean N-A_T = 2295.7±4.6 µmol kg^{-1} and n = 67 for 2005–2017; not shown). In the coastal zones off Brittany, the A_T is also highly variable (Salt et al., 2016; Gac et al., 2021), ranging between 2150 and 2386 µmol kg^{-1} (Fig. 12).

An interesting signal is the progressive increase in A_T in the Mediterranean Sea. The positive A_T trend of +0.53

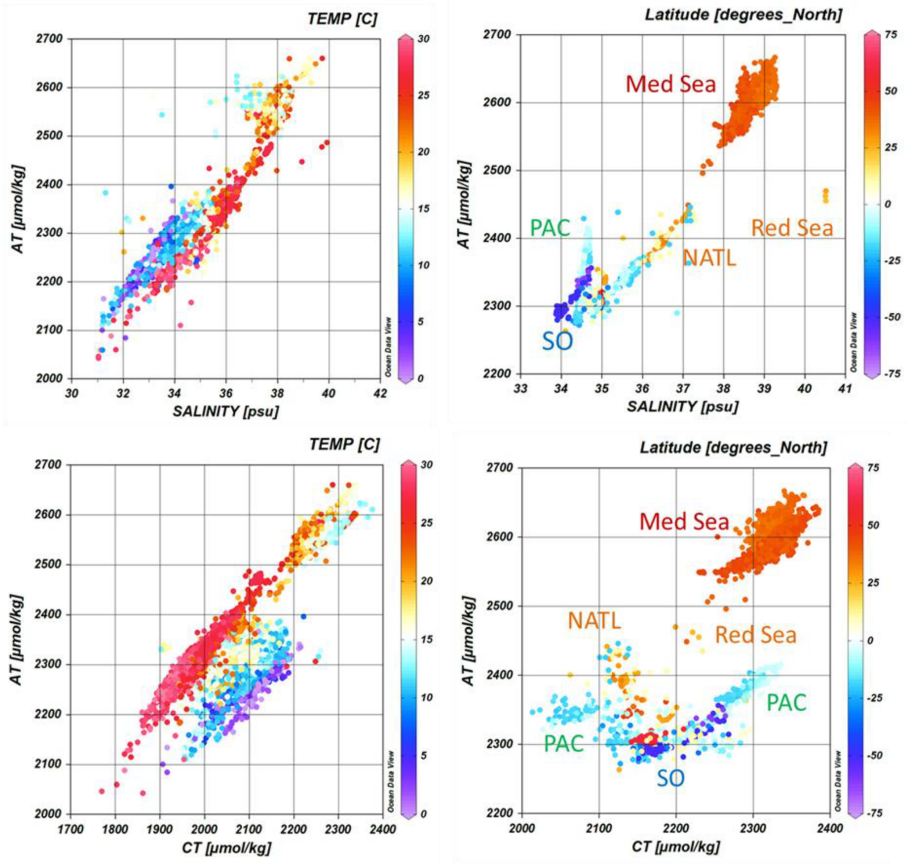

Figure 8. Relationships between A_T and salinity (upper panels) and between A_T and C_T (lower panels) for samples in surface waters (0–10 m and sea surface salinity (SSS) >31) (left) and in the water column below 100 m (right). Only data with Flag 2 are presented. The color scales correspond to the temperature (left) or the latitude (right). The following data locations are identified: Mediterranean Sea (Med Sea), Red Sea, tropical Pacific (PAC), North Atlantic (NATL) and Southern Ocean (SO). The figure was produced with ODV (Schlitzer, 2018).

(±0.11) µmol kg^{-1} yr^{-1} ($n = 538$) in 1998–2019 in the offshore region was also observed at the SOMLIT-Point-B coastal station in 2007–2015, although with a faster increase of +2.08 (±0.19) µmol kg^{-1} yr^{-1} (Kapsenberg et al., 2017). Close to the DYFAMED site, at SOMLIT-Point-B station, the A_T trend was not linked to temporal salinity changes, as a positive N-A_T trend was also reported, +0.52 (±0.07) µmol kg^{-1} yr^{-1} (not shown). Based on data from the PERLE cruises in 2018–2021, a significant increase in A_T was also identified in the eastern Mediterranean Sea (Wimart-Rousseau et al., 2021). Along with the increase in C_T and the warming, the A_T increase would impact on the fCO_2, the air–sea CO_2 fluxes and pH temporal changes (Merlivat et al., 2018). Processes explaining the A_T increase in the Mediterranean Sea are still unexplained and deserve further investigation (Coppola et al., 2019).

As expected, because of the anthropogenic CO_2 uptake, the C_T concentrations increased in most regions (Fig. 12, Table 6). This is identified in the Indian Ocean (in the subtropical and the high-latitude sectors), in the Mediterranean Sea and in coastal waters off Brittany. However, the signal is more complex in the NASPG. As previously shown, the C_T trend in the NASPG depends on the season and decade (Metzl et al., 2010; Reverdin et al., 2018; Fröb et al., 2019; Leseurre et al., 2020). Here, we selected only the data in January–February from the SURATLANT cruises, leading to a C_T trend of +0.72 (±0.17) µmol kg^{-1} yr^{-1}. Compared with the regions further north, the C_T trend in the NASPG is about half the C_T trends of +1.44 (±0.23) µmol kg^{-1} yr^{-1} observed in the Iceland Sea (Olafsson et al., 2009) or +1.48 (±0.22) µmol kg^{-1} yr^{-1} at station M in the Norwegian Sea (Skjelvan et al., 2022).

In the coastal zones off Brittany, although there are large seasonal and interannual variabilities (Gac et al., 2021), an annual C_T trend of +1.72 (±0.28) µmol kg^{-1} yr^{-1} is detected over 10 years (2009–2019). The same is observed in the Mediterranean Sea, where the C_T offshore trend of +0.69 (±0.18) µmol kg^{-1} yr^{-1} is low compared with what was observed in the coastal zone (SOMLIT-Point-B, +2.97 (±0.20) µmol kg^{-1} yr^{-1}; Kapsenberg et al., 2017).

In the southern Indian Ocean, C_T concentrations also increased in both the subtropics and at high latitudes,

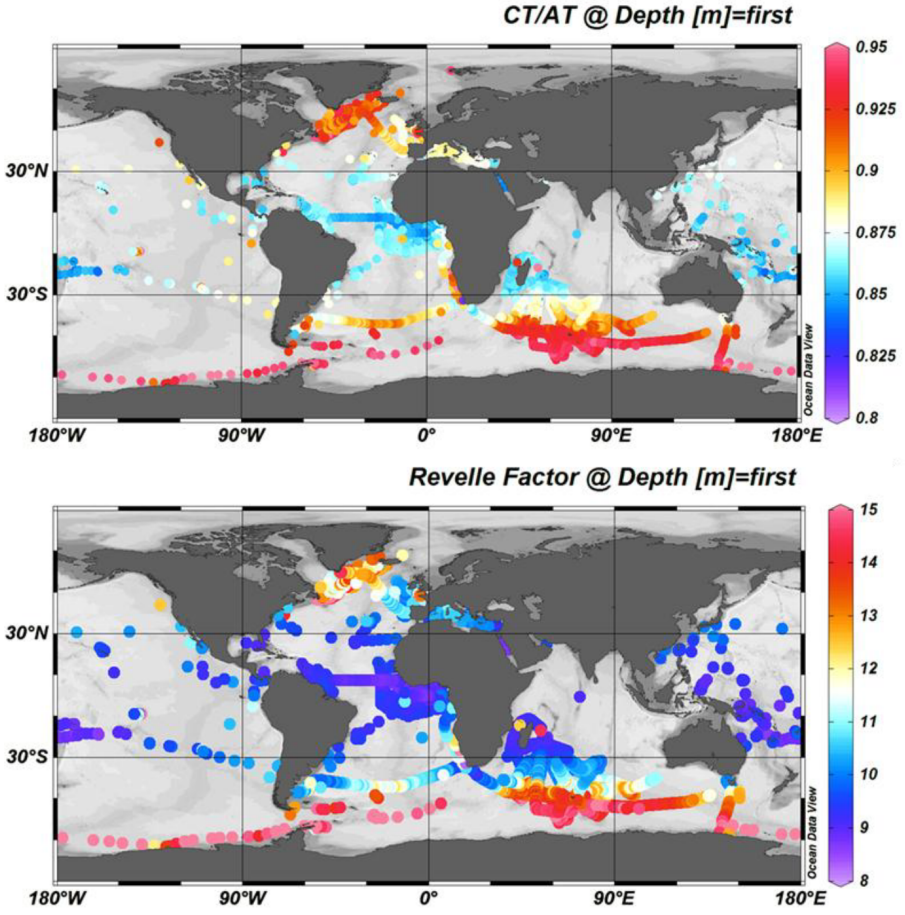

Figure 9. Distribution of the C_T/A_T ratio (top) and the Revelle factor (bottom) in surface waters (0–10 m). Only data with Flag 2 were used. The figure was produced with ODV (Schlitzer, 2018).

Table 6. Trend in C_T ($\mu mol\,kg^{-1}\,yr^{-1}$) and the corresponding standard error in five selected regions where data were available for more than 10 years (data are shown in Fig. 12). The projects/cruises for the selection of the data in each domain are indicated.

Region (acronym)	Period	C_T trend ($\mu mol\,kg^{-1}\,yr^{-1}$)	Season	Projects/Cruises
North Atlantic (NASPG)	1994–2014	+0.72	January–February	SURATLANT
Indian subtropical (IO-SBT)	1998–2018	+0.65	January–February	OISO
Indian south (IO-POOZ)	1998–2018	+0.67	January–February	OISO
Ligurian Sea (MED)	1998–2019	+0.68	All seasons	DYFAMED, BOUSSOLE, MOOSE-GE
Coast of Brittany (BRIT)	2008–2019	+1.72	All seasons	Brest, Roscoff, ECOSCOPA, Penzé

two regions where the primary productivity is relatively low (an oligotrophic regime in the subtropics and a high-nutrient–low-chlorophyll regime, HNLC, south of the polar front). With the data selected for austral summer (January–February), the C_T trends appeared almost similar in these two regions, around $+0.65\,\mu mol\,kg^{-1}\,yr^{-1}$ (Table 6).

Finally, in the equatorial Atlantic, the selected data around 0°–10° W highlighted the large variability linked to the oceanic circulation. Detecting a C_T trend as well as a possible link to anthropogenic carbon uptake, at least with the data available in 2005–2017, appears to be intricate, as has been previously discussed for the period 2006–2013 (Lefèvre et al., 2016). However, the signal of the C_T increase is better identified north or south of the Equator in the eastern tropical Atlantic sector (Lefèvre et al., 2021).

In the water column, A_T and C_T data from dedicated cruises were used to evaluate the anthropogenic CO_2 (C_{ant}) distribution and pH change since the preindustrial era

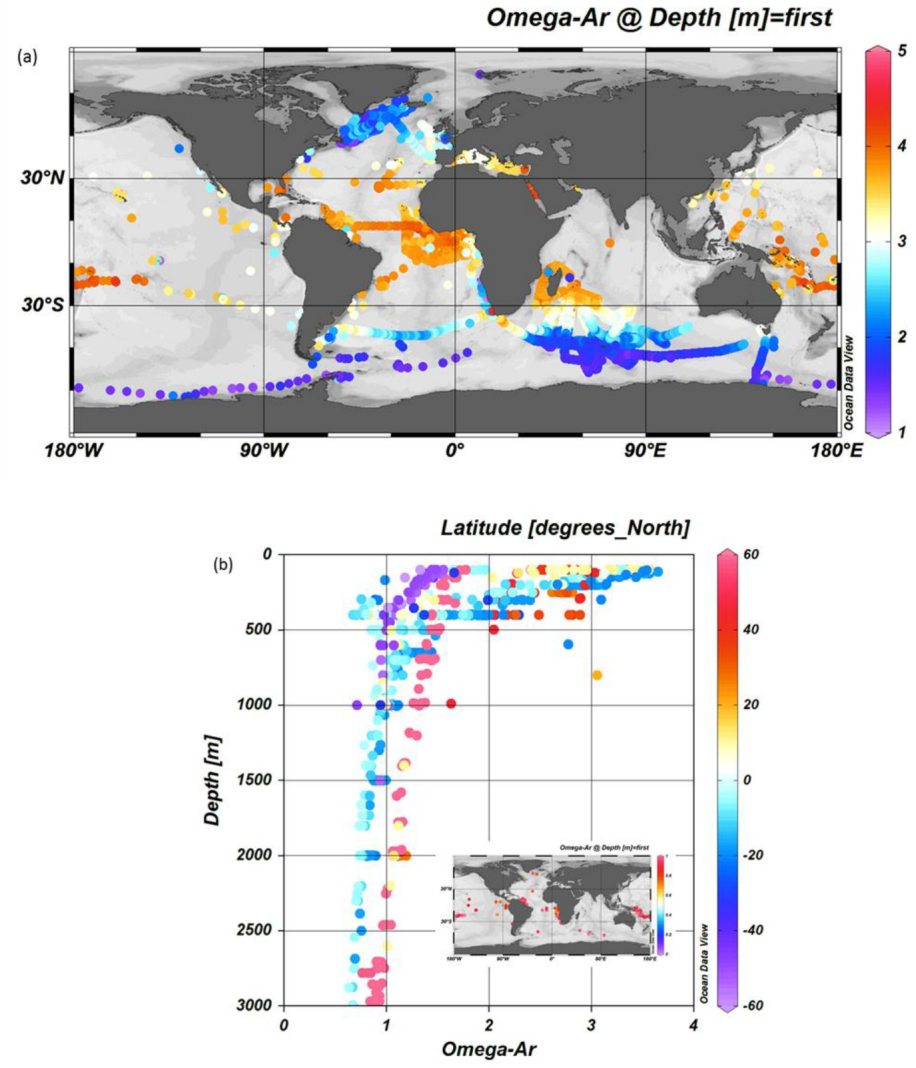

Figure 10. Panel **(a)** shows the distribution of the aragonite saturation state (Ω-Ar) in surface waters (0–10 m). Only data with Flag 2 were used. Panel **(b)** presents depth profiles (100–3000 m) of Ω-Ar at few locations in the tropical Pacific, Atlantic and Southern oceans. Stations where undersaturation is detected (Ω-Ar <1) at depth are identified in the inset map. The figure was produced with ODV (Schlitzer, 2018).

(e.g., PANDORA cruise – Ganachaud et al., 2017; OUTPACE cruise – Wagener et al., 2018a; SOMBA cruise – Keraghel et al., 2020). Time series at DYFAMED station also enabled us to investigate the temporal variability in C_T, A_T and C_{ant} in the water column (Touratier and Goyet, 2009; Coppola et al., 2020; Fourrier et al., 2022). As an example of the observed temporal variations at depth, we selected the data in the 950–1050 m layer in the Ligurian Sea from different cruises (Fig. 13). At that depth, both A_T and C_T present some large anomalies that were especially noticeable in 2013 (lower A_T and C_T in February 2013, DEWEX cruise) and in 2018 (higher A_T and C_T in May 2018, MOOSE-GE cruise), with the latter probably being linked to an episodic convective process that occurred in winter 2018 (Fourrier et al., 2022; Coppola et al., 2023). During the strong convection event in 2013, the positive anomalies of A_T and C_T were mostly identified in the upper layers (Fig. 12c).

In this region, the long-term increase in A_T indicates that, in addition to the anthropogenic CO_2 signal, other processes are at play to explain the rapid C_T trend of $+1.20$ (± 0.12) µmol kg^{-1} yr^{-1} at depth compared with that observed at the surface (Fig. 12). The signal at depth is probably linked to the variations in the deep convection and mixing with Levantine Intermediate Water (LIW; Margirier et al., 2020) that has higher A_T and C_T concentrations. The long-term increase in A_T and C_T at depth (here at 1000 m; Fig. 13) was also observed below 2000 m (Coppola et al., 2020); this signal should be investigated using a dedicated analysis with other properties (e.g., O_2 and nutrients), following Fourrier

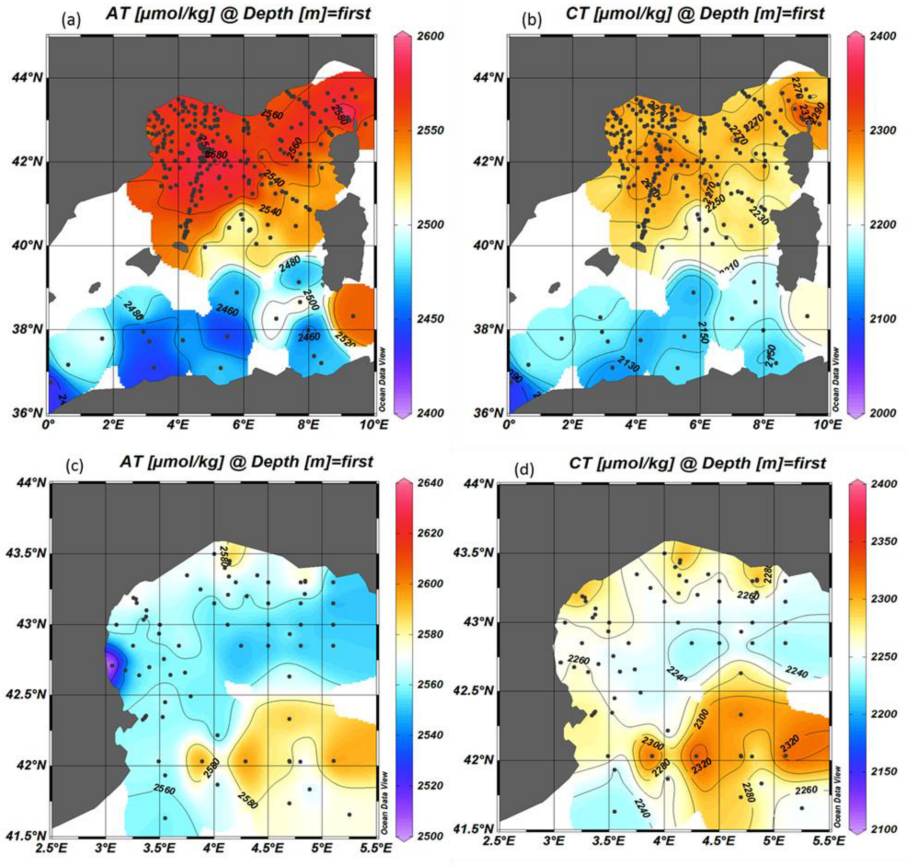

Figure 11. Distribution (in µmol kg^{-1}) of A_T **(a)** and C_T **(b)** in surface waters of the western Mediterranean Sea (0–10 m) from all data for 1998–2019. A detailed distribution (in µmol kg^{-1}) of A_T **(c)** and C_T **(d)** in surface waters of the Gulf of Lion is also given for the 2010–2011 period only (the CARBORHONE, CASCADE, LATEX, MOLA and MOOSE-GE cruises). The figure was produced with ODV (Schlitzer, 2018).

et al. (2022) for the 2012–2020 period, and a larger dataset in the Mediterranean Sea (e.g., GLODAP).

6 Using A_T and C_T data to validate observations from autonomous instruments

The dataset presented in this synthesis would also offer interesting observations to validate properties (A_T and C_T) derived from Biogeochemical-Argo (BGC-Argo) floats equipped with pH sensors (e.g., Bushinsky et al., 2019; Mazloff et al., 2023; Mignot et al., 2023). The water-column in situ A_T and C_T data obtained during the Antarctic Circumpolar Expedition (ACE) in 2016–2017 were collected at a location where Southern Ocean Carbon and Climate Observations and Modeling (SOCCOM) floats were launched (Walton and Thomas, 2018). A SOCCOM float (WMO ID 5905069) was launched on 11 January 2017 at 55° S, 96° E, south of the polar front in the southern Indian Ocean. The pH, temperature and salinity data from the float were then used to derive A_T and C_T profiles (here using a multiple linear regression, MLR, algorithm; Williams et al., 2016, 2017). In the top layers, the discrete ACE data (Fig. 14) present large variability in the A_T and C_T concentrations that is not captured in the records derived from the float (the MLR method somehow smoothed the profiles). However, given the uncertainty in reconstructed A_T from float data (5.6 µmol kg^{-1}), the average values in the first 100 m were almost identical ($A_{T-ACE} = 2285.1$ (±4.4) µmol kg^{-1} and $A_{T-float} = 2278.3$ (±0.7) µmol kg^{-1}; $C_{T-ACE} = 2139.7$ (±9.2) µmol kg^{-1} and $C_{T-float} = 2141.1$ (±3.2) µmol kg^{-1}). Moreover, below 200 m, profiles from the float are coherent compared to the A_T and C_T measurements (Fig. 14). This is encouraging with respect to using float data to explore the seasonal variability in A_T and C_T in the Southern Ocean (e.g., Williams et al., 2018; Johnson et al., 2022) and to estimate anthropogenic CO_2 in the water column in this sector (Fig. 14). Here, the C_{ant} concentrations were calculated below 200 m (corresponding to the temperature minimum of the winter in the Southern Ocean and using the TrOCA – Tracer combining Oxygen, inorganic Carbon and total Alkalinity – method; Touratier et al., 2007). The float data suggest that C_{ant} concentrations are positive down to about 1000 m,

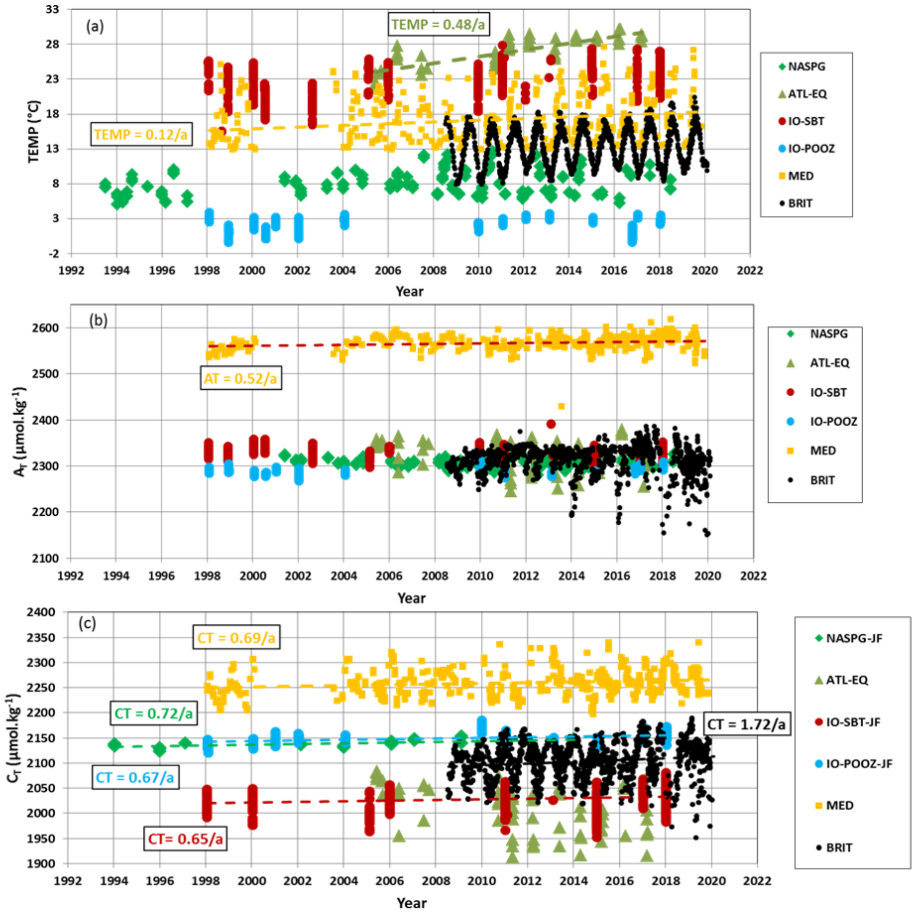

Figure 12. Time series of **(a)** sea-surface temperature (°C), **(b)** A_T (µmol kg^{-1}) and **(c)** C_T (µmol kg^{-1}) in six regions: the North Atlantic subpolar gyre (NASPG, 1993–2018, green diamond), the equatorial Atlantic (ATL-EQ, 2005–2017, green triangle), the Indian subtropical sector (IO-SBT, red circle) and high-latitude sector (IO-POOZ, blue circle) (1998–2018), the Ligurian Sea (MED, 1998–2019, orange square), and times series' stations in the coastal zones off Brittany (BRIT, period 2008–2019, black dots). Trends (dashed lines and values) are shown when relevant for the discussion (C_T trends listed in Table 6).

with maximum values in the subsurface. In 2017, the mean C_{ant} concentration at 200 m was 49.1 (±9.0) µmol kg^{-1}. Below that depth, C_{ant} decreased to +29.8 (±8.5) µmol kg^{-1} in the 300–400 m layer. To complement the C_{ant} inventories based on the GLODAP data product (e.g., Gruber et al., 2019), C_{ant} estimates derived from BGC-Argo floats, as evaluated here in the Southern Ocean, could be applied in other locations, as was previously tested in the North Pacific (Li et al., 2019).

In surface water, as the A_T derived from the float data are deduced using MLR or LIAR (locally interpolated A_T regression) methods (Williams et al., 2017; Carter et al., 2016), the A_T data in the SNAPO-CO2 synthesis could also be used to identify A_T anomalies that are not always captured from floats. This is particularly relevant in coccolithophore bloom areas when low A_T concentrations and high pCO_2 are observed (e.g., Balch et al., 2016, in the Southern Ocean; Robertson et al., 1994, in the North Atlantic).

7 Data availability

Data presented in this study are available from SEANOE: https://www.seanoe.org (last access: 22 December 2023), https://doi.org/10.17882/95414 (Metzl et al., 2023).

8 Summary and suggestions

The ocean data synthesized in this product are based on measurements of A_T and C_T performed between 1993 and 2022 with an accuracy of ±4 µmol kg^{-1}. The product offers a large dataset of A_T and C_T for the Global Ocean and regional biogeochemical studies. It includes more than 44 400 surface and water-column observations in all oceanic basins, in the Mediterranean Sea, in the coastal zones, near coral reefs and in rivers. For the open ocean, this complements the SOCAT and GLODAP data products (Bakker et al., 2016; Lauvset et al., 2022). For the coastal sites, this also complements the synthesis of coastal time series only done around North

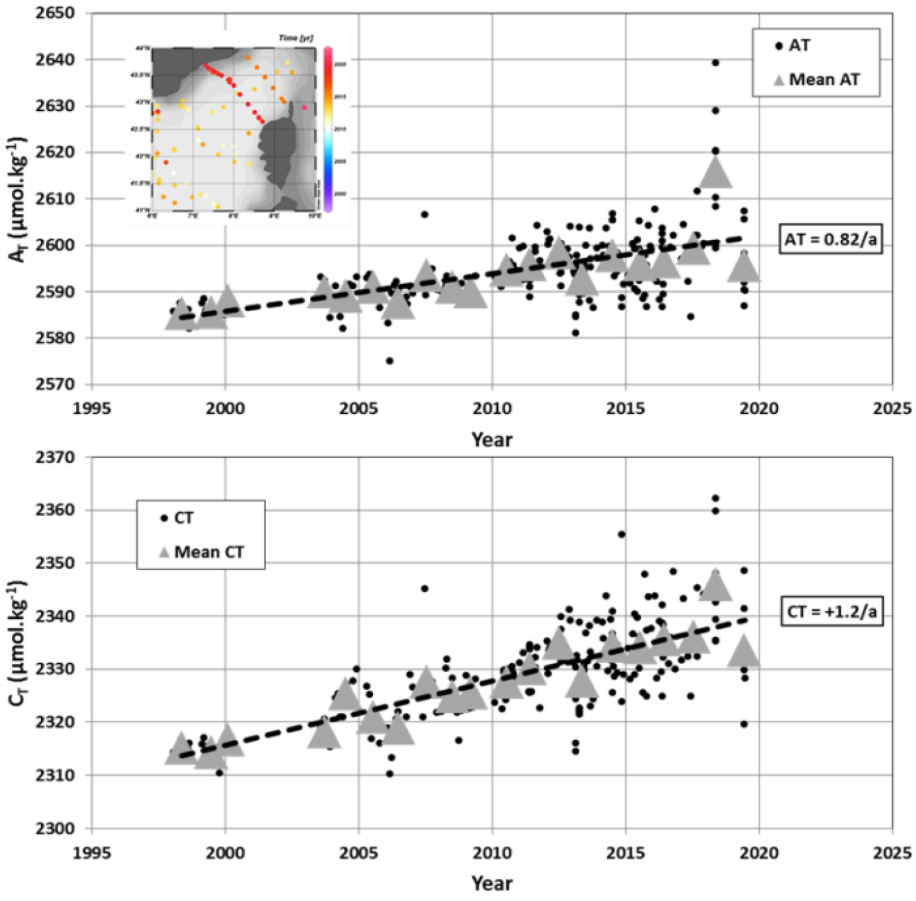

Figure 13. Time series of A_T (µmol kg^{-1}) and C_T (µmol kg^{-1}) in the Ligurian Sea (1998–2019) in the 950–1050 m layer. The annual mean (gray triangles) was calculated from all data each year (black dots). The trends (dashed line) based on the annual mean are +0.82 (±0.15) µmol kg^{-1} yr^{-1} for A_T and +1.20 (±0.12) µmol kg^{-1} yr^{-1} for C_T. In this layer, selected data are from the ANTARES, CASCADE, DEWEX, DYFAMED, MOOSE-GE and PEACETIME cruises (location of stations shown in the inset map produced with ODV; Schlitzer, 2018).

America (Fassbender et al., 2018; Jiang et al., 2021; OCADS, 2023).

The SNAPO-CO2 dataset enables the investigation of seasonal variations to decadal trends in A_T and C_T in various oceanic provinces. In regions where data are available for more than 2 decades in surface water (North Atlantic, Ligurian Sea, southern Indian Ocean and coastal regions), all time series show an increase in C_T. Apart from in the Mediterranean Sea, A_T appears relatively constant over time, although the A_T content presents significant interannual variability, such as in the NASPG or in the coastal zones, including near the Congo and Amazon river plumes.

This dataset represents independent data for the validation of reconstructed A_T or C_T fields using various methods (e.g., Rödenbeck et al., 2013, 2015; Sauzède et al., 2017; Turk et al., 2017; Bittig et al., 2018; Broullón et al., 2019, 2020; Land et al., 2019; Keppler et al., 2020; Fourier et al., 2020; Gregor and Gruber, 2021; Sims et al., 2023). It is also useful to validate Earth system models (ESMs) that currently present bias with respect to the reproduction of the seasonal cycle of C_T and A_T due to the inadequate representation of biogeochemical cycles, including the coupling of biological and physical processes (e.g., Pilcher et al., 2015; Mongwe et al., 2018; Lerner et al., 2021). This should be resolved in order to ensure confident future projections of productivity, ocean acidification and the responses of the marine ecosystems (e.g., Kwiatowski et al., 2020). Recall that ocean biogeochemical global models (OBGMs) or ESMs calculate pCO_2 from A_T–C_T pairs and that the simulated annual CO_2 flux might be correct when compared to observations but for the wrong reasons (e.g., Goris et al., 2018; Lerner et al., 2021). For example, it has been shown that biases in A_T in ESMs lead to an overestimation of the oceanic fCO_2 trend and, thus, uncertainty when predicting the oceanic anthropogenic CO_2 uptake (Lebehot et al., 2019). The simulated seasonal cycle of fCO_2 is also uncertain in ESMs, especially at high latitudes (e.g., Joos et al., 2023). Thus, it is important

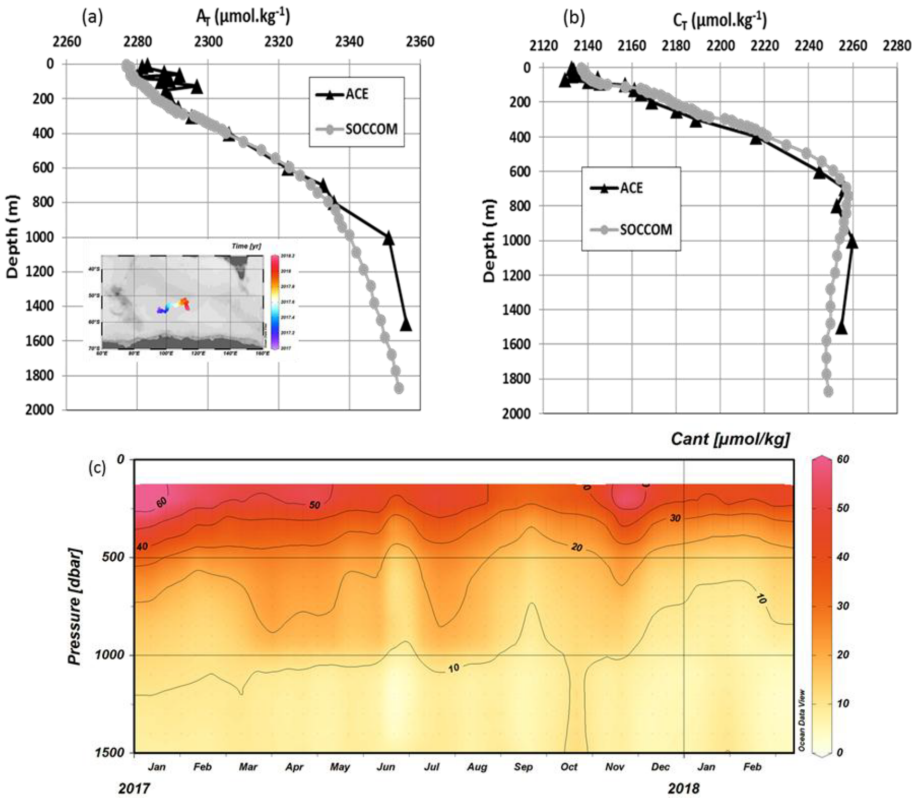

Figure 14. Profiles of **(a)** A_T (µmol kg^{-1}) and **(b)** C_T (µmol kg^{-1}) observed at station ACE-20 (55° S, 95° E; 11 January 2017, black triangles) compared with the profiles deduced from the SOCCOM float (WMO code 5905069) launched at that location (first data on 12 January 2017, gray circles). The location and drift of the float in 2017–2018 are shown on the inset map. Panel **(c)** presents a Hovmöller section (pressure versus time) of anthropogenic CO_2 concentrations (C_{ant}, in µmol kg^{-1}) estimated from the float data (A_T, C_T, O_2, T) below 200 m (period from January 2017 to February 2018). The section was produced with ODV (Schlitzer, 2018).

to attempt to validate ESMs with A_T and C_T data, such as undertaken in this synthesis.

This dataset would also serve to validate autonomous platforms capable of measuring pH and fCO_2 variables and, along with SOCAT and GLODAP datasets, provides an additional reference dataset for the development and validation of regional biogeochemical models for simulating air–sea CO_2 fluxes. It is also essential for training and validating neural networks capable of predicting variables in the carbonate system, thereby enhancing observations of marine CO_2 at different spatial and temporal scales.

The data presented here are available online on the SEANOE server (Metzl et al., 2023, https://doi.org/10.17882/95414) and are divided in two files: one for the Global Ocean and one for the Mediterranean Sea. The sources of the original datasets (DOI) and their associated references are listed in the Supplement (Tables S3, S4). We invite users to comment on any anomalies that have not been detected or to suggest any potential misqualifications of data in the present product (e.g., data probably good, although assigned Flag 3, probably wrong). The SNAPO-CO2 dataset will be regularly updated on the SEANOE data server (with new observations), controlled and archived.

Supplement. The supplement related to this article is available online at: https://doi.org/10.5194/essd-16-89-2024-supplement.

Author contributions. NM prepared the data synthesis, the figures and wrote the draft of the manuscript with contributions from all authors. JF measured the discrete samples (from 2014 on) with help from CM and CLM and also prepared the individual reports for each project. NM and JF pre-qualified the discrete A_T and C_T data. CLM and NM are co-investigators of the ongoing OISO project and qualified the underway A_T and C_T data from OISO and CLIMEPARSES cruises. All authors have reviewed the manuscript and contributed to one or more of the following: organizing cruises, sample collection and/or data qualification.

Competing interests. The contact author has declared that none of the authors has any competing interests.

Disclaimer. Publisher's note: Copernicus Publications remains neutral with regard to jurisdictional claims made in the text, published maps, institutional affiliations, or any other geographical representation in this paper. While Copernicus Publications makes every effort to include appropriate place names, the final responsibility lies with the authors.

Acknowledgements. The A_T and C_T data presented in this study were measured at the SNAPO-CO2 facility (Service National d'Analyse des Paramètres Océaniques du CO_2), which is housed by the LOCEAN laboratory and part of the OSU ECCE Terra at the Sorbonne University and INSU/CNRS analytical services. Support from INSU/CNRS, OSU ECCE Terra and LOCEAN, is gratefully acknowledged as well as support from different French "Services nationaux d'Observations", such as OISO/CARAUS, SOMLIT, PIRATA, SSS and MOOSE. We thank the research infrastructure ICOS (Integrated Carbon Observation System) France for funding a large part of the analyses. We thank the French oceanographic fleet ("Flotte océanographique française") for financial and logistic support for most cruises listed in this synthesis and for the OISO program (https://campagnes.flotteoceanographique.fr/series/228/, last access: 22 December 2023). We acknowledge the MOOSE (Mediterranean Ocean Observing System for the Environment, https://campagnes.flotteoceanographique.fr/series/235/fr/, last access: 22 December 2023) program coordinated by CNRS-INSU and the research infrastructure ILICO (CNRS-IFREMER). AWIPEV-CO2 was supported by the Coastal Observing System for Northern and Arctic Seas (COSYNA), the two Helmholtz large-scale infrastructure projects ACROSS and MOSES, the French Polar Institute Paul-Émile Victor (IPEV), and the European Union Horizon 2020 Research and Innovation projects Jericho-Next (grant nos. 871153 and 951799), INTAROS (grant no. 727890) and FACE-IT (grant no. 869154). The BOUSSOLE project was funded by the Centre National d'Etudes Spatiales (CNES) and the European Space Agency (ESA ESRIN, contract no. 4000119096/17/I-BG), and the first 3 years of the CO_2 time series at that site were funded by the French Agence Nationale de la Recherche (ANR). The EURECA^4-OA cruise was also supported by the EUREC4A-OA JPI Ocean and Climate program. We thank the Tara Ocean Foundation and many institutes and funding agencies for supporting Tara cruises since 2009. The OISO program was supported by the French institutes INSU (Institut National des Sciences de l'Univers) and IPEV (Institut Polaire Paul-Émile Victor), OSU Ecce Terra (at Sorbonne Université), and the French program SOERE/GreatGases. The CLIM-EPARSES cruise was supported by TAAF (Terres Australes et ANtarctiques Françaises), Fondation du Prince Albert II de Monaco, IRD, OSU Ecce Terra, CNRS, MNHN, LOCEAN and LSCE laboratory. Data from the float launched during the ACE cruise were made freely available by the Southern Ocean Carbon and Climate Observations and Modeling (SOCCOM) project funded by the National Science Foundation, Division of Polar Programs (NSF PLR, award no. 1425989), supplemented by NASA, and by the international Argo program and the NOAA programs that contribute to it. The Argo program is part of the Global Ocean Observing System (https://doi.org/10.17882/42182, Argo, 2023, http://argo.jcommops.org, last access: 22 December 2023). We thank Frédéric Merceur (IFREMER) for preparing the page and data availability on SEANOE. We thank Patrick Raimbault (retired, formerly at MIO, Marseille) for managing the MOOSE project until 2019. We thank all colleagues and students who participated in the cruises and carefully collected the precious seawater samples. We warmly acknowledge our colleague Christian Brunet (retired) for his supportive help with the analysis since the start of the SNAPO-CO2 service facility. We would like to pay tribute to our late colleague Frédéric Diaz who contributed to the LATEX cruise in 2010. We thank the editor Xingchen Wang for managing this manuscript and Marta Álvarez and a (more or less) anonymous reviewer for their suggestions that helped to improve this article.

Financial support. This research has been supported by the Institut national des sciences de l'Univers (SA/SNAPO-CO2).

Review statement. This paper was edited by Xingchen Wang and reviewed by Marta Álvarez and one anonymous referee.

References

Álvarez, M., Catalá, T. S., Civitarese, G., Coppola, L., Hassoun, A. E. R., Ibello, V., Lazzari, P., Lefèvre, D., Macías, D., Santinelli, C., and Ulses, C.: Chapter 11 – Mediterranean Sea general biogeochemistry, Editor(s): Katrin Schroeder, Jacopo Chiggiato, Oceanography of the Mediterranean Sea, Elsevier, 387–451, https://doi.org/10.1016/B978-0-12-823692-5.00004-2, 2023.

Argo: Argo float data and metadata from Global Data Assembly Centre (Argo GDAC), SEANOE [data set], https://doi.org/10.17882/42182, 2023.

Bakker, D. C. E., Pfeil, B., Smith, K., Hankin, S., Olsen, A., Alin, S. R., Cosca, C., Harasawa, S., Kozyr, A., Nojiri, Y., O'Brien, K. M., Schuster, U., Telszewski, M., Tilbrook, B., Wada, C., Akl, J., Barbero, L., Bates, N. R., Boutin, J., Bozec, Y., Cai, W.-J., Castle, R. D., Chavez, F. P., Chen, L., Chierici, M., Currie, K., de Baar, H. J. W., Evans, W., Feely, R. A., Fransson, A., Gao, Z., Hales, B., Hardman-Mountford, N. J., Hoppema, M., Huang, W.-J., Hunt, C. W., Huss, B., Ichikawa, T., Johannessen, T., Jones, E. M., Jones, S. D., Jutterström, S., Kitidis, V., Körtzinger, A., Landschützer, P., Lauvset, S. K., Lefèvre, N., Manke, A. B., Mathis, J. T., Merlivat, L., Metzl, N., Murata, A., Newberger, T., Omar, A. M., Ono, T., Park, G.-H., Paterson, K., Pierrot, D., Ríos, A. F., Sabine, C. L., Saito, S., Salisbury, J., Sarma, V. V. S. S., Schlitzer, R., Sieger, R., Skjelvan, I., Steinhoff, T., Sullivan, K. F., Sun, H., Sutton, A. J., Suzuki, T., Sweeney, C., Takahashi, T., Tjiputra, J., Tsurushima, N., van Heuven, S. M. A. C., Vandemark, D., Vlahos, P., Wallace, D. W. R., Wanninkhof, R., and Watson, A. J.: An update to the Surface Ocean CO_2 Atlas (SOCAT version 2), Earth Syst. Sci. Data, 6, 69–90, https://doi.org/10.5194/essd-6-69-2014, 2014.

Bakker, D. C. E., Pfeil, B., Landa, C. S., Metzl, N., O'Brien, K. M., Olsen, A., Smith, K., Cosca, C., Harasawa, S., Jones, S. D., Nakaoka, S., Nojiri, Y., Schuster, U., Steinhoff, T., Sweeney, C., Takahashi, T., Tilbrook, B., Wada, C., Wanninkhof, R., Alin, S.

R., Balestrini, C. F., Barbero, L., Bates, N. R., Bianchi, A. A., Bonou, F., Boutin, J., Bozec, Y., Burger, E. F., Cai, W.-J., Castle, R. D., Chen, L., Chierici, M., Currie, K., Evans, W., Featherstone, C., Feely, R. A., Fransson, A., Goyet, C., Greenwood, N., Gregor, L., Hankin, S., Hardman-Mountford, N. J., Harlay, J., Hauck, J., Hoppema, M., Humphreys, M. P., Hunt, C. W., Huss, B., Ibánhez, J. S. P., Johannessen, T., Keeling, R., Kitidis, V., Körtzinger, A., Kozyr, A., Krasakopoulou, E., Kuwata, A., Landschützer, P., Lauvset, S. K., Lefèvre, N., Lo Monaco, C., Manke, A., Mathis, J. T., Merlivat, L., Millero, F. J., Monteiro, P. M. S., Munro, D. R., Murata, A., Newberger, T., Omar, A. M., Ono, T., Paterson, K., Pearce, D., Pierrot, D., Robbins, L. L., Saito, S., Salisbury, J., Schlitzer, R., Schneider, B., Schweitzer, R., Sieger, R., Skjelvan, I., Sullivan, K. F., Sutherland, S. C., Sutton, A. J., Tadokoro, K., Telszewski, M., Tuma, M., van Heuven, S. M. A. C., Vandemark, D., Ward, B., Watson, A. J., and Xu, S.: A multidecade record of high-quality fCO_2 data in version 3 of the Surface Ocean CO_2 Atlas (SOCAT), Earth Syst. Sci. Data, 8, 383–413, https://doi.org/10.5194/essd-8-383-2016, 2016.

Bakker, D. C. E., Alin, S. R., Bates, N. R., Becker, M., Feely, R. A., Gritzalis, T., Jones, S. D., Kozyr, A., Lauvset, S. K., Metzl, N., Munro, D. R., Nakaoka, S.-I., Nojiri, Y., O'Brien, K., Olsen, A., Pierrot, D., Rehder, G., Steinhoff, T., Sutton, A., Sweeney, C., Tilbrook, B., Wada, C., Wanninkhof, R., and SOCAT contributors: An alarming decline in the ocean CO_2 observing capacity, https://www.socat.info (last access: 22 December 2023), 2023.

Balch, W. M., Bates, N. R., Lam, P. J., Twining, B. S., Rosengard, S. Z., Bowler, B. C., Drapeau, D. T., Garley, R., Lubelczyk, L. C., Mitchell, C., and Rauschenberg S.: Factors regulating the Great Calcite Belt in the Southern Ocean and its biogeochemical significance, Global Biogeochem. Cy., 30, 1124–1144, https://doi.org/10.1002/2016GB005414, 2016.

Bates, N., Astor, Y., Church, M., Currie, K., Dore, J., González-Dávila, M., Lorenzoni, L., Muller-Karger, F., Olafsson, J., and Santa-Casiano, M.: A Time-Series View of Changing Ocean Chemistry Due to Ocean Uptake of Anthropogenic CO_2 and Ocean Acidification, Oceanography, 27, 126–141, https://doi.org/10.5670/oceanog.2014.16, 2014.

Beaufort, L., Probert, I., de Garidel-Thoron, T., Bendif, E. M., Ruiz-Pino, D., Metzl, N., Goyet, C., Buchet, N., Coupel, P., Grelaud, M., Rost, B., Rickaby, R. E. M., and de Vargas C.: Sensitivity of coccolithophores to carbonate chemistry and ocean acidification, Nature, 476, 80–83, https://doi.org/10.1038/nature10295, 2011.

Bittig, H. C., Steinhoff, T., Claustre, H., Fiedler, B., Williams, N. L., Sauzède, R., Körtzinger, A., and Gattuso, J.-P.: An Alternative to Static Climatologies: Robust Estimation of Open Ocean CO_2 Variables and Nutrient Concentrations From T, S, and O_2 Data Using Bayesian Neural Networks, Front. Mar. Sci., 5, 328, https://doi.org/10.3389/fmars.2018.00328, 2018.

Bockmon, E. E. and Dickson, A. G.: An inter-laboratory comparison assessing the quality of seawater carbon dioxide measurements, Mar. Chem., 171, 36–43, https://doi.org/10.1016/j.marchem.2015.02.002, 2015.

Bosse, A., Testor, P., Mayot, N., Prieur, L., D'Ortenzio, F., Mortier, L., Le Goff, H., Gourcuff, C., Coppola, L., Lavigne, H., and Raimbault, P.: A submesoscale coherent vortex in the Ligurian Sea: From dynamical barriers to biological implications, J. Geophys. Res.-Oceans, 122, 6196–6217, https://doi.org/10.1002/2016JC012634, 2017.

Bozec, Y., Merlivat, L., Baudoux, A.-C., Beaumont, L., Blain, S., Bucciarelli, E., Danguy, T., Grossteffan, E., Guillot, A., Guillou, J., Répécaud, M., and Tréguer, P.: Diurnal to inter-annual dynamics of pCO_2 recorded by a CARIOCA sensor in a temperate coastal ecosystem (2003–2009), Mar. Chem., 126, 13–26, https://doi.org/10.1016/j.marchem.2011.03.003, 2011.

Broullón, D., Pérez, F. F., Velo, A., Hoppema, M., Olsen, A., Takahashi, T., Key, R. M., Tanhua, T., González-Dávila, M., Jeansson, E., Kozyr, A., and van Heuven, S. M. A. C.: A global monthly climatology of total alkalinity: a neural network approach, Earth Syst. Sci. Data, 11, 1109–1127, https://doi.org/10.5194/essd-11-1109-2019, 2019.

Broullón, D., Pérez, F. F., Velo, A., Hoppema, M., Olsen, A., Takahashi, T., Key, R. M., Tanhua, T., Santana-Casiano, J. M., and Kozyr, A.: A global monthly climatology of oceanic total dissolved inorganic carbon: a neural network approach, Earth Syst. Sci. Data, 12, 1725–1743, https://doi.org/10.5194/essd-12-1725-2020, 2020.

Bushinsky, S. M., Landschützer, P., Rödenbeck, C., Gray, A. R., Baker, D., Mazloff, M. R., Resplandy L., Johnson K. S., and Sarmiento, J. L.: Reassessing Southern Ocean air-sea CO_2 flux estimates with the addition of biogeochemical float observations, Global Biogeochem. Cy., 33, 1370–1388, https://doi.org/10.1029/2019GB006176, 2019.

Canesi, M., Douville, E., Montagna, P., Taviani, M., Stolarski, J., Bordier, L., Dapoigny, A., Coulibaly, G. E. H., Simon, A.-C., Agelou, M., Fin, J., Metzl, N., Iwankow, G., Allemand, D., Planes, S., Moulin, C., Lombard, F., Bourdin, G., Troublé, R., Agostini, S., Banaigs, B., Boissin, E., Boss, E., Bowler, C., de Vargas, C., Flores, M., Forcioli, D., Furla, P., Gilson, E., Galand, P. E., Pesant, S., Sunagawa, S., Thomas, O., Thurber, R. V., Voolstra, C. R., Wincker, P., Zoccola, D., and Reynaud, S.: Differences in carbonate chemistry upregulation of long-lived reef-building corals, Sci. Rep. 13, 11589, https://doi.org/10.1038/s41598-023-37598-9, 2023.

Caniaux, G., Giordani, H., Redelsperger, J.-L., Guichard, F., Key, E., and Wade, M.: Coupling between the Atlantic cold tongue and the West African monsoon in boreal spring and summer, J. Geophys. Res., 119, C04003, https://doi.org/10.1029/2010JC006570, 2011.

Carter, B. R., Williams, N. L., Gray, A. R., and Feely, R. A.: Locally interpolated alkalinity regression for global alkalinity estimation, Limnol. Oceanogr.-Meth., 14, 268–277, https://doi.org/10.1002/lom3.10087, 2016.

Chen, H., Haumann, F. A., Talley, L. D., Johnson, K. S., and Sarmiento, J. L.: The deep ocean's carbon exhaust, Global Biogeochem. Cy., 36, e2021GB007156, https://doi.org/10.1002/essoar.10507757.1, 2022.

Cheng, L. J., Abraham, J., Zhu, J., Trenberth, K. E., Fasullo, J., Boyer, T., Locarnini, R., Zhang, B., Yu, F. J., Wan, L. Y., Chen, X. R., Song, X. Z., Liu, Y. L., and Mann, M. E.: Record-setting ocean warmth continued in 2019, Adv. Atmos. Sci, 37, 137–142, https://doi.org/10.1007/s00376-020-9283-7, 2020.

Claustre, H., Johnson, K. S., and Takeshita, Y.: Observing the Global Ocean with Biogeochemical-Argo, Annu. Rev. Mar. Sci., 12, 23–48, https://doi.org/10.1146/annurev-marine-010419-010956, 2020.

Copin-Montégut, C.: Alkalinity and carbon budgets in the Mediterranean Sea, Global Biogeochem. Cy., 7, 915–925, 1993.

Copin-Montégut, C. and Bégovic, M.: Distributions of carbonate properties and oxygen along the water column (0–2000 m) in the central part of the NW Mediterranean Sea (Dyfamed site): influence of the winter vertical mixing on air–sea CO_2 and O_2 exchanges, Deep-Sea Res. Pt. II, 49, 2049–2066, https://doi.org/10.1016/S0967-0645(02)00027-9,2002.

Coppola, L., Raimbault, P., Mortier, L., and Testor, P.: Monitoring the environment in the northwestern Mediterranean Sea, Eos, 100, https://doi.org/10.1029/2019EO125951, 2019.

Coppola, L., Boutin, J., Gattuso, J.-P., Lefèvre, D., and Metzl, N.: The Carbonate System in the Ligurian Sea, in: The Mediterranean Sea in the Era of Global Change: Evidence from 30 years of multidisciplinary study of the Ligurian Sea, edited by: Migon, C., Nival, P., and Sciandra, A., vol. 1, chap. 4, ISTE Science Publishing LTD, London, UK, 79–104, ISBN 9781786304285, https://doi.org/10.1002/9781119706960.ch4, 2020.

Coppola, L., Fourrier, M., Pasqueron de Fommervault, O., Poteau, A., Riquier, E. D., and Béguery, L.: Highresolution study of the air-sea CO_2 flux and net community oxygen production in the Ligurian Sea by a fleet of gliders, Front. Mar. Sci., 10, 1233845, https://doi.org/10.3389/fmars.2023.1233845, 2023.

Corbière, A., Metzl, N., Reverdin, G., Brunet, C., and Takahashi, T.: Interannual and decadal variability of the oceanic carbon sink in the North Atlantic subpolar gyre, Tellus B, 59, 168–179, https://doi.org/10.1111/j.1600-0889.2006.00232.x, 2007.

De Carlo, E. H., Mousseau, L., Passafiume, O., Drupp, P., and Gattuso J.-P.: Carbonate chemistry and air-sea CO_2 flux in a NW Mediterranean bay over a four-year period: 2007–2011, Aquat. Geochem., 19, 399–442, https://doi.org/10.1007/s10498-013-9217-4, 2013.

Dickson, A. G., Sabine, C. L., and Christian, J. R.: Guide to best practices for ocean CO_2 measurements, North Pacific Marine Science Organization, Sidney, British Columbia, 191, https://doi.org/10.25607/OBP-1342, 2007.

Doney, S. C., Fabry, V. J., Feely, R. A., and Kleypas, J. A.: Ocean acidification: The other CO_2 problem, Annu. Rev. Mar. Sci., 1, 169–192, https://doi.org/10.1146/annurev.marine.010908.163834, 2009.

Doney, S. C., Busch, D. S., Cooley, S. R., and Kroeker, K. J.: The Impacts of Ocean Acidification on Marine Ecosystems and Reliant Human Communities, Annu. Rev. Env. Resour., 45, 83–112, https://doi.org/10.1146/annurev-environ-012320-083019, 2020.

Douville, E., Bourdin, G., Lombard, F., Gorsky, G., Fin, J., Metzl, N., Pesant, S., and Tara Pacific Consortium: Seawater carbonate chemistry dataset collected during the Tara Pacific Expedition 2016–2018, PANGAEA [data set], https://doi.org/10.1594/PANGAEA.944420, 2022.

Edmond, J. M.: High precision determination of titration alkalinity and total carbon dioxide content of sea water by potentiometric titration, Deep-Sea Res., 17, 737–750, https://doi.org/10.1016/0011-7471(70)90038-0, 1970.

Eyring, V., Righi, M., Lauer, A., Evaldsson, M., Wenzel, S., Jones, C., Anav, A., Andrews, O., Cionni, I., Davin, E. L., Deser, C., Ehbrecht, C., Friedlingstein, P., Gleckler, P., Gottschaldt, K.-D., Hagemann, S., Juckes, M., Kindermann, S., Krasting, J., Kunert, D., Levine, R., Loew, A., Mäkelä, J., Martin, G., Mason, E., Phillips, A. S., Read, S., Rio, C., Roehrig, R., Senftleben, D., Sterl, A., van Ulft, L. H., Walton, J., Wang, S., and Williams, K. D.: ESMValTool (v1.0) – a community diagnostic and performance metrics tool for routine evaluation of Earth system models in CMIP, Geosci. Model Dev., 9, 1747–1802, https://doi.org/10.5194/gmd-9-1747-2016, 2016.

Fabry, V. J., Seibel, B. A., Feely, R. A., and Orr, J. C.: Impacts of ocean acidification on marine fauna and ecosystem processes, ICES J. Mar. Sci., 65, 414–432, https://doi.org/10.1093/icesjms/fsn048, 2008.

Fassbender, A. J., Sabine, C. L., and Palevsky, H. I.: Nonuniform ocean acidification and attenuation of the ocean carbon sink, Geophys. Res. Lett., 44, 8404–8413, https://doi.org/10.1002/2017GL074389, 2017.

Fassbender, A. J., Alin, S. R., Feely, R. A., Sutton, A. J., Newton, J. A., Krembs, C., Bos, J., Keyzers, M., Devol, A., Ruef, W., and Pelletier, G.: Seasonal carbonate chemistry variability in marine surface waters of the US Pacific Northwest, Earth Syst. Sci. Data, 10, 1367–1401, https://doi.org/10.5194/essd-10-1367-2018, 2018.

Feely, R. A., Sabine, C. L., Byrne, R. H., Millero, F. J., Dickson, A. G., Wanninkhof, R., Murata, A., Miller, L. A., and Greeley, D.: Decadal changes in the aragonite and calcite saturation state of the Pacific Ocean, Global Biogeochem. Cy., 26, GB3001, https://doi.org/10.1029/2011GB004157, 2012.

Feely, R. A., Jiang, L.-Q., Wanninkhof, R., Carter, B. R., Alin, S. R., Bednaršek, N., and Cosca, C. E.: Acidification of the global surface ocean: What we have learned from observations, Oceanography, 36, 120–129, https://doi.org/10.5670/oceanog.2023.222, 2023.

Fleury, E., Petton, S., Benabdelmouna, A., and Pouvreau, S., (coord.): Observatoire national du cycle de vie de l'huître creuse en France, Rapport annuel ECOSCOPA 2022, R.INT.BREST RBE/PFOM/PI 2023-1, https://archimer.ifremer.fr/doc/00840/95240/102991.pdf, last access: 22 December 2023.

Fourrier, M., Coppola, L., Claustre, H., D'Ortenzio, F., Sauzède, R., and Gattuso, J.-P.: A regional neural network approach to estimate water-column nutrient concentrations and carbonate system variables in the Mediterranean Sea: CANYON-MED, Front. Mar. Sci., 7, 620, https://doi.org/10.3389/fmars.2020.00620, 2020.

Fourrier, M., Coppola, L., D'Ortenzio, F., Migon, C., and Gattuso, J.-P.: Impact of intermittent convection in the northwestern Mediterranean Sea on oxygen content, nutrients, and the carbonate system, J. Geophys. Res.-Oceans, 127, e2022JC018615, https://doi.org/10.1029/2022JC018615, 2022.

Friedlingstein, P., O'Sullivan, M., Jones, M. W., Andrew, R. M., Gregor, L., Hauck, J., Le Quéré, C., Luijkx, I. T., Olsen, A., Peters, G. P., Peters, W., Pongratz, J., Schwingshackl, C., Sitch, S., Canadell, J. G., Ciais, P., Jackson, R. B., Alin, S. R., Alkama, R., Arneth, A., Arora, V. K., Bates, N. R., Becker, M., Bellouin, N., Bittig, H. C., Bopp, L., Chevallier, F., Chini, L. P., Cronin, M., Evans, W., Falk, S., Feely, R. A., Gasser, T., Gehlen, M., Gkritzalis, T., Gloege, L., Grassi, G., Gruber, N., Gürses, Ö., Harris, I., Hefner, M., Houghton, R. A., Hurtt, G. C., Iida, Y., Ilyina, T., Jain, A. K., Jersild, A., Kadono, K., Kato, E., Kennedy, D., Klein Goldewijk, K., Knauer, J., Korsbakken, J. I., Landschützer, P., Lefèvre, N., Lindsay, K., Liu, J., Liu, Z., Marland, G., Mayot, N., McGrath, M. J., Metzl, N., Monacci, N. M., Munro, D. R., Nakaoka, S.-I., Niwa, Y., O'Brien, K., Ono, T., Palmer, P. I., Pan, N., Pierrot, D., Pocock, K., Poulter, B., Resplandy, L., Robertson, E., Rödenbeck, C., Rodriguez, C., Rosan, T. M., Schwinger,

J., Séférian, R., Shutler, J. D., Skjelvan, I., Steinhoff, T., Sun, Q., Sutton, A. J., Sweeney, C., Takao, S., Tanhua, T., Tans, P. P., Tian, X., Tian, H., Tilbrook, B., Tsujino, H., Tubiello, F., van der Werf, G. R., Walker, A. P., Wanninkhof, R., Whitehead, C., Willstrand Wranne, A., Wright, R., Yuan, W., Yue, C., Yue, X., Zaehle, S., Zeng, J., and Zheng, B.: Global Carbon Budget 2022, Earth Syst. Sci. Data, 14, 4811–4900, https://doi.org/10.5194/essd-14-4811-2022, 2022.

Fröb, F., Olsen, A., Becker, M., Chafik, L., Johannessen, T., Reverdin, G., and Omar, A.: Wintertime fCO_2 variability in the subpolar North Atlantic since 2004, Geophys. Res. Lett., 46, 1580–1590, https://doi.org/10.1029/2018GL080554, 2019.

Gac, J.-P., Marrec, P., Cariou, T., Guillerm, C., Macé, E., Vernet, M., and Bozec, Y.: Cardinal buoys: An opportunity for the study of air-sea CO_2 fluxes in coastal ecosystems, Front. Mar. Sci., 7, 712, https://doi.org/10.3389/fmars.2020.00712, 2020.

Gac, J.-P., Marrec, P., Cariou, T., Grosstefan, E., Macé, E., Rimmelin-Maury, P., Vernet, M., and Bozec, Y.: Decadal Dynamics of the CO_2 System and Associated Ocean Acidification in Coastal Ecosystems of the North East Atlantic Ocean, Front. Mar. Sci., 8, 688008, https://doi.org/10.3389/fmars.2021.688008, 2021.

Ganachaud, A., Cravatte, S., Sprintall, J., Germineaud, C., Alberty, M., Jeandel, C., Eldin, G., Metzl, N., Bonnet, S., Benavides, M., Heimburger, L.-E, Lefèvre, J., Michael, S., Resing, J., Quéroué, F., Sarthou, G., Rodier, M., Berthelot, H., Baurand, F., Grelet, J., Hasegawa, T., Kessler, W., Kilepak, M., Lacan, F., Privat, E., Send, U., Van Beek, P., Souhaut, M., and Sonke, J. E.:. The Solomon Sea: its circulation, chemistry, geochemistry and biology explored during two oceanographic cruises, Elem. Sci. Anth., 5, 33, https://doi.org/10.1525/elementa.221, 2017.

Gattuso, J.-P., Magnan, A., Billé, R., Cheung, W. W. L., Howes, E. L., Joos, F., Allemand, D., Bopp, L., Cooley, S., Eakin, M., Hoegh-Guldberg, O., Kelly, R. P., Pörtner, H.-O., Rogers, A. D., Baxter, J. M., Laffoley, D., Osborn, D., Rankovic, A., Rochette, J., Sumaila, U. R., Treyer, S., and Turley, C.: Contrasting futures for ocean and society from different anthropogenic CO_2 emissions scenarios, Science, 349, aac4722, https://doi.org/10.1126/science.aac4722, 2015.

Gattuso, J.-P., Alliouane, S., and Fischer, P.: High-frequency, year-round time series of the carbonate chemistry in a high-Arctic fjord (Svalbard), Earth Syst. Sci. Data, 15, 2809–2825, https://doi.org/10.5194/essd-15-2809-2023, 2023.

Gemayel, E., Hassoun, A. E. R., Benallal, M. A., Goyet, C., Rivaro, P., Abboud-Abi Saab, M., Krasakopoulou, E., Touratier, F., and Ziveri, P.: Climatological variations of total alkalinity and total dissolved inorganic carbon in the Mediterranean Sea surface waters, Earth Syst. Dynam., 6, 789–800, https://doi.org/10.5194/esd-6-789-2015, 2015.

Golbol M., Boutin J., Merlivat L., Vellucci, V., and Antoine, D.: Dissolved Inorganic Carbon and Total Alkalinity sampled at Boussole site in the Medditerranean Sea, SEANOE [data set], https://doi.org/10.17882/71911, 2020.

Goris, N., Tjiputra, J. F., Olsen, A., Schwinger, J., Lauvset, S. K., and Jeansson, E.: Constraining projection-based estimates of the future North Atlantic carbon uptake, J. Climate, 31, 3959–3978, https://doi.org/10.1175/JCLI-D-17-0564.1, 2018.

Goyet, C., Beauverger, C., Brunet, C., and Poisson, A.: Distribution of carbon dioxide partial pressure in surface waters of the Southwest Indian Ocean, Tellus B, 43, 1–11, https://doi.org/10.3402/tellusb.v43i1.15242, 1991.

Gregor, L. and Gruber, N.: OceanSODA-ETHZ: a global gridded data set of the surface ocean carbonate system for seasonal to decadal studies of ocean acidification, Earth Syst. Sci. Data, 13, 777–808, https://doi.org/10.5194/essd-13-777-2021, 2021.

Gruber, N., Clement, D., Carter, B. R., Feely, R. A., van Heuven, S., Hoppema, M., Ishii, M., Key, R. M., Kozyr, A., Lauvset, S. K., Lo Monaco, C. , Mathis, J. T., Murata, A., Olsen, A., Perez, F. F., Sabine, C. L., Tanhua, T., and Wanninkhof, R.: The oceanic sink for anthropogenic CO_2 from 1994 to 2007, Science, 363, 1193–1199, https://doi.org/10.1126/science.aau5153, 2019.

Hagens, M. and Middelburg, J. J.: Attributing seasonal pH variability in surface ocean waters to governing factors, Geophys. Res. Lett., 43, 12528–12537, https://doi.org/10.1002/2016GL071719, 2016.

Henson, S. A., Painter, S. C., Holliday, N. P., Stinchcombe, M. C., and Giering, S. L. C.: Unusual subpolar North Atlantic phytoplankton bloom in 2010: Volcanic fertilization or North Atlantic Oscillation?, J. Geophys. Res.-Oceans, 118, 4771–4780, https://doi.org/10.1002/jgrc.20363, 2013.

Hoegh-Guldberg, O., Mumby, P. J., Hooten, A. J., Steneck, R. S., Greenfield, P., Gomez, E., Harvell, C. D., Sale, P. F., Edwards, A. J., Caldeira, K., Knowlton, N., Eakin, C. M., Iglesias-Prieto, R., Muthiga, N., Bradbury, R. H., Dubi, A., and Hatziolos, M. E.: Coral reefs under rapid climate change and ocean acidification, Science, 14, 1737–1742, https://doi.org/10.1126/science.1152509, 2007.

Hood, E. M. and Merlivat, L.: Annual to interannual variations of fCO_2 in the northwestern Mediterranean Sea: Results from hourly measurements made by CARIOCA buoys, 1995–1997, J. Mar. Res., 59, 113–131, https://elischolar.library.yale.edu/journal_of_marine_research/2386 (last access: 22 December 2023), 2001.

Howes, E., Stemmann, L., Assailly, C., Irisson, J.-O., Dima, M., Bijma, J., and Gattuso, J.-P.: Pteropod time series from the North Western Mediterranean (1967–2003): impacts of pH and climate variability, Mar. Ecol. Prog. Ser., 531, 193–206, https://doi.org/10.3354/meps11322, 2015.

Howes, E. L., Eagle, R., Gattuso, J.-P., and Bijma, J.: Comparison of Mediterranean pteropod shell biometrics and ultrastructure from historical (1910 and 1921) and present day (2012) samples provides baseline for monitoring effects of global change, PLoS ONE, 12, e0167891, https://doi.org/10.1371/journal.pone.0167891, 2017.

IPCC: Changing Ocean, Marine Ecosystems, and Dependent Communities, in: The Ocean and Cryosphere in a Changing Climate, Cambridge University Press, 447–588, https://doi.org/10.1017/9781009157964.007, 2022.

Jiang, L.-Q., Feely, R. A., Carter, B. R., Greeley, D. J., Gledhill, D. K., and Arzayus K. M.: Climatological distribution of aragonite saturation state in the global oceans, Global Biogeochem. Cy., 29, 1656–1673, https://doi.org/10.1002/2015GB005198, 2015.

Jiang, L.-Q., Carter, B. R., Feely, R. A., Lauvset, S. K., and Olsen, A.: Surface ocean pH and buffer capacity: past, present and future, Sci. Rep., 9, 18624, https://doi.org/10.1038/s41598-019-55039-4, 2019.

Jiang, L.-Q., Feely, R. A., Wanninkhof, R., Greeley, D., Barbero, L., Alin, S., Carter, B. R., Pierrot, D., Featherstone, C., Hooper,

J., Melrose, C., Monacci, N., Sharp, J. D., Shellito, S., Xu, Y.-Y., Kozyr, A., Byrne, R. H., Cai, W.-J., Cross, J., Johnson, G. C., Hales, B., Langdon, C., Mathis, J., Salisbury, J., and Townsend, D. W.: Coastal Ocean Data Analysis Product in North America (CODAP-NA) – an internally consistent data product for discrete inorganic carbon, oxygen, and nutrients on the North American ocean margins, Earth Syst. Sci. Data, 13, 2777–2799, https://doi.org/10.5194/essd-13-2777-2021, 2021.

Jiang, L.-Q., Dunne, J., Carter, B. R., Tjiputra, J. F., Terhaar, J., Sharp, J. D., Olsen, A., Alin, S., Bakker, D. C. E., Feely, R. A., Gattuso, J.-P., Hogan, P., Ilyina, T., Lange, N., Lauvset, S. K., Lewis, E. R., Lovato, T., Palmieri, J., Santana-Falcón, Y., Schwinger, J., Séférian, R., Strand, G., Swart, N., Tanhua, T., Tsujino, H., Wanninkhof, R., Watanabe, M., Yamamoto, A., and Ziehn, T.: Global surface ocean acidification indicators from 1750 to 2100, J. Adv. Model. Earth Sy., 15, e2022MS003563, https://doi.org/10.1029/2022MS003563, 2023a.

Jiang, L. Q., Kozyr, A., Relph, J. M., Ronje, E. I., Kamb, L., Burger, E., Myer, J., Nguyen, L., and Arzayus, K. M.: The Ocean Carbon and Acidification Data System, Sci. Data, 10, 136, https://doi.org/10.1038/s41597-023-02042-0, 2023b.

Jiang, Z.-P., Tyrrell, T., Hydes, D. J., Dai, M., and Hartman, S. E.: Variability of alkalinity and the alkalinity-salinity relationship in the tropical and subtropical surface ocean, Global Biogeochem. Cy., 28, 729–742, https://doi.org/10.1002/2013GB004678, 2014.

Johnson, K. S., Mazloff, M. R., Bif, M. B., Takeshita, Y., Jannasch, H. W., Maurer, T. L., Plant, J. N., Verdy, A., Walz, P. M., Riser, S. C., and Talley, L. D.: Carbon to nitrogen uptake ratios observed across the Southern Ocean by the SOCCOM profiling float array, J. Geophys. Res.-Oceans, 127, e2022JC018859, https://doi.org/10.1029/2022JC018859, 2022.

Joos, F., Hameau, A., Frölicher, T. L., and Stephenson, D. B.: Anthropogenic attribution of the increasing seasonal amplitude in surface ocean pCO_2, Geophys. Res. Lett., 50, e2023GL102857, https://doi.org/10.1029/2023GL102857, 2023.

Joyce, T. and Corry, C. (Eds.): Requirements for WOCE Hydrographic Programme Data Reporting, WHPO Publication 90-1 Revision 2, WOCE Report 67/91, Woods Hole, Mass., USA, https://cchdo.github.io/hdo-assets/documentation/manuals/pdf/90_1/title.pdf (last access: 22 December 2023), 1994.

Kapsenberg, L., Alliouane, S., Gazeau, F., Mousseau, L., and Gattuso, J.-P.: Coastal ocean acidification and increasing total alkalinity in the northwestern Mediterranean Sea, Ocean Sci., 13, 411–426, https://doi.org/10.5194/os-13-411-2017, 2017.

Keppler, L., Landschützer, P., Gruber, N., Lauvset, S. K., and Stemmler, I.: Seasonal carbon dynamics in the near-global ocean, Global Biogeochem. Cy., 34, e2020GB006571, https://doi.org/10.1029/2020GB006571, 2020.

Keppler, L., Landschützer, P., Lauvset, S. K., and Gruber, N.: Recent trends and variability in the oceanic storage of dissolved inorganic carbon, Global Biogeochem. Cy., 37, e2022GB007677, https://doi.org/10.1029/2022GB007677, 2023.

Keraghel, M. A., Louanchi, F., Zerrouki, M., Kaci, M. A., Aït-Ameur, N., Labaste, M., Legoff, H., Taillandier, V., Harid, R., and Mortier, L.: Carbonate system properties and anthropogenic carbon inventory in the Algerian Basin during SOMBA cruise (2014): Acidification estimate, Mar. Chem., 221, 103783, https://doi.org/10.1016/j.marchem.2020.103783, 2020.

Key, R. M., Kozyr, A., Sabine, C. L., Lee, K., Wanninkhof, R., Bullister, J. L., Feely, R. A., Millero, F. J., Mordy, C., and Peng, T. H.: A global ocean carbon climatology: Results from Global Data Analysis Project (GLODAP), Global Biogeochem. Cy., 18, GB4031, https://doi.org/10.1029/2004GB002247, 2004.

Key, R. M., Tanhua, T., Olsen, A., Hoppema, M., Jutterström, S., Schirnick, C., van Heuven, S., Kozyr, A., Lin, X., Velo, A., Wallace, D. W. R., and Mintrop, L.: The CARINA data synthesis project: introduction and overview, Earth Syst. Sci. Data, 2, 105–121, https://doi.org/10.5194/essd-2-105-2010, 2010.

Khatiwala, S., Tanhua, T., Mikaloff Fletcher, S., Gerber, M., Doney, S. C., Graven, H. D., Gruber, N., McKinley, G. A., Murata, A., Ríos, A. F., and Sabine, C. L.: Global ocean storage of anthropogenic carbon, Biogeosciences, 10, 2169–2191, https://doi.org/10.5194/bg-10-2169-2013, 2013.

Kitidis, V., Shutler, J. D., Ashton, I., Warren, M., Brown, I., Findlay, H., Hartman, S. E., Sanders, R., Humphreys, M., Kivimäe, C., Greenwood, N., Hull, T., Pearce, D., McGrath, T., Stewart, B. M., Walsham, P., McGovern, E., Bozec, Y., Gac, J.-P., van Heuven, S., Hoppema, M., Schuster, U., Johannessen, T., Omar, A., Lauvset, S. K., Skjelvan, I., Olsen, A., Steinhoff, T., Körtzinger, A., Becker, M., Lefèvre, N., Diverrès, D., Gkritzalis, T., Cattrijsse, A., Petersen, W., Voynova, Y., Chapron, B., Grouazel, A., Land, P. E., Sharples, J., and Nightingale, P. D.: Winter weather controls net influx of atmospheric CO_2 on the north-west European shelf, Sci. Rep., 9, 20153, https://doi.org/10.1038/s41598-019-56363-5, 2019.

Koffi, U., Lefèvre, N., Kouadio, G., and Boutin, J.: Surface CO_2 parameters and air-sea CO_2 fluxes distribution in the eastern equatorial Altantic Ocean, J. Marine Syst., 82, 135–144, https://doi.org/10.1016/j.jmarsys.2010.04.010, 2010.

Koseki, S., Tjiputra, J., Fransner, F., Crespo, Lander R., and Keenlyside, N. S.: Disentangling the impact of Atlantic Niño on sea-air CO_2 flux, Nat. Commun., 14, 3649, https://doi.org/10.1038/s41467-023-38718-9, 2023.

Kwiatkowski, L., Torres, O., Bopp, L., Aumont, O., Chamberlain, M., Christian, J. R., Dunne, J. P., Gehlen, M., Ilyina, T., John, J. G., Lenton, A., Li, H., Lovenduski, N. S., Orr, J. C., Palmieri, J., Santana-Falcón, Y., Schwinger, J., Séférian, R., Stock, C. A., Tagliabue, A., Takano, Y., Tjiputra, J., Toyama, K., Tsujino, H., Watanabe, M., Yamamoto, A., Yool, A., and Ziehn, T.: Twenty-first century ocean warming, acidification, deoxygenation, and upper-ocean nutrient and primary production decline from CMIP6 model projections, Biogeosciences, 17, 3439–3470, https://doi.org/10.5194/bg-17-3439-2020, 2020.

Land, P. E., Findlay, H. S., Shutler, J. D., Ashton, I. G., Holding, T., Grouazel, A., Girard-Ardhuin, F., Reul, N., Piolle, J. F., Chapron, B., and Quilfen, Y.: Optimum satellite remote sensing of the marine carbonate system using empirical algorithms in the global ocean, the Greater Caribbean, the Amazon Plume and the Bay of Bengal, Remote Sens. Environ., 235, 111469, https://doi.org/10.1016/j.rse.2019.111469, 2019.

Lauvset, S. K., Gruber, N., Landschützer, P., Olsen, A., and Tjiputra, J.: Trends and drivers in global surface ocean pH over the past 3 decades, Biogeosciences, 12, 1285–1298, https://doi.org/10.5194/bg-12-1285-2015, 2015.

Lauvset, S. K., Carter, B. R., Perez, F. F., Jiang, L.-Q., Feely, R. A., Velo, A., and Olsen, A.: Processes Driving Global Interior Ocean

pH Distribution, Global Biogeochem. Cy., 34, e2019GB006229, https://doi.org/10.1029/2019GB006229, 2020.

Lauvset, S. K., Lange, N., Tanhua, T., Bittig, H. C., Olsen, A., Kozyr, A., Álvarez, M., Becker, S., Brown, P. J., Carter, B. R., Cotrim da Cunha, L., Feely, R. A., van Heuven, S., Hoppema, M., Ishii, M., Jeansson, E., Jutterström, S., Jones, S. D., Karlsen, M. K., Lo Monaco, C., Michaelis, P., Murata, A., Pérez, F. F., Pfeil, B., Schirnick, C., Steinfeldt, R., Suzuki, T., Tilbrook, B., Velo, A., Wanninkhof, R., Woosley, R. J., and Key, R. M.: An updated version of the global interior ocean biogeochemical data product, GLODAPv2.2021, Earth Syst. Sci. Data, 13, 5565–5589, https://doi.org/10.5194/essd-13-5565-2021, 2021.

Lauvset, S. K., Lange, N., Tanhua, T., Bittig, H. C., Olsen, A., Kozyr, A., Alin, S., Álvarez, M., Azetsu-Scott, K., Barbero, L., Becker, S., Brown, P. J., Carter, B. R., da Cunha, L. C., Feely, R. A., Hoppema, M., Humphreys, M. P., Ishii, M., Jeansson, E., Jiang, L.-Q., Jones, S. D., Lo Monaco, C., Murata, A., Müller, J. D., Pérez, F. F., Pfeil, B., Schirnick, C., Steinfeldt, R., Suzuki, T., Tilbrook, B., Ulfsbo, A., Velo, A., Woosley, R. J., and Key, R. M.: GLODAPv2.2022: the latest version of the global interior ocean biogeochemical data product, Earth Syst. Sci. Data, 14, 5543–5572, https://doi.org/10.5194/essd-14-5543-2022, 2022.

Lebehot, A. D., Halloran, P. R., Watson, A. J., McNeall, D., Ford, D. A., Landschützer, P., Lauvset, S. K., and Schuster, U.: Reconciling Observation and Model Trends in North Atlantic Surface CO_2, Global Biogeochem. Cy., 33, 1204–1222, https://doi.org/10.1029/2019GB006186, 2019.

Lee, K., Wanninkhof, R., Feely, R. A., Millero, F. J., and Peng, T.-H.: Global relationships of total inorganic carbon with temperature and nitrate in surface seawater, Global Biogeochem. Cy., 14, 979–994, https://doi.org/10.1029/1998GB001087, 2000.

Lee, K., Tong, L. T., Millero, F. J., Sabine, C. L., Dickson, A. G., Goyet, C., Park, G. H., Wanninkhof, R., Feely, R. A., and Key, R. M.: Global relationships of total alkalinity with salinity and temperature in surface waters of the world's oceans, Geophys. Res. Lett., 33, L19605, doi10.1029/2006GL027207, 2006.

Lefèvre, N. and Merlivat, L.: Carbon and oxygen net community production in the eastern tropical Atlantic estimated from a moored buoy, Global Biogeochem. Cy., 26, GB1009, https://doi.org/10.1029/2010GB004018, 2012.

Lefèvre, N., Guillot, A., Beaumont, L., and Danguy, T.: Variability of fCO_2 in the Eastern Tropical Atlantic from a moored buoy, J. Geophys. Res.-Oceans, 113, C01015, https://doi.org/10.1029/2007JC004146, 2008.

Lefèvre, N., Diverres, D., and Gallois, F.: Origin of CO_2 undersaturation in the western tropical Atlantic, Tellus B, 62, 595–607, https://doi.org/10.1111/j.1600-0889.2010.00475.x, 2010.

Lefèvre, N., Veleda, D., Araujo, M., and Caniaux, G.: Variability and trends of carbon parameters at a time series in the eastern tropical Atlantic, Tellus B, 68, 30305, https://doi.org/10.3402/tellusb.v68.30305, 2016.

Lefèvre, N., Mejia, C., Khvorostyanov, D., Beaumont, L., and Koffi, U.: Ocean Circulation Drives the Variability of the Carbon System in the Eastern Tropical Atlantic, Oceans, 2021, 126–148, https://doi.org/10.3390/oceans2010008, 2021.

Le Quéré, C., Moriarty, R., Andrew, R. M., Canadell, J. G., Sitch, S., Korsbakken, J. I., Friedlingstein, P., Peters, G. P., Andres, R. J., Boden, T. A., Houghton, R. A., House, J. I., Keeling, R. F., Tans, P., Arneth, A., Bakker, D. C. E., Barbero, L., Bopp, L., Chang, J., Chevallier, F., Chini, L. P., Ciais, P., Fader, M., Feely, R. A., Gkritzalis, T., Harris, I., Hauck, J., Ilyina, T., Jain, A. K., Kato, E., Kitidis, V., Klein Goldewijk, K., Koven, C., Landschützer, P., Lauvset, S. K., Lefèvre, N., Lenton, A., Lima, I. D., Metzl, N., Millero, F., Munro, D. R., Murata, A., Nabel, J. E. M. S., Nakaoka, S., Nojiri, Y., O'Brien, K., Olsen, A., Ono, T., Pérez, F. F., Pfeil, B., Pierrot, D., Poulter, B., Rehder, G., Rödenbeck, C., Saito, S., Schuster, U., Schwinger, J., Séférian, R., Steinhoff, T., Stocker, B. D., Sutton, A. J., Takahashi, T., Tilbrook, B., van der Laan-Luijkx, I. T., van der Werf, G. R., van Heuven, S., Vandemark, D., Viovy, N., Wiltshire, A., Zaehle, S., and Zeng, N.: Global Carbon Budget 2015, Earth Syst. Sci. Data, 7, 349–396, https://doi.org/10.5194/essd-7-349-2015, 2015.

Lerner, P., Romanou, A., Kelley, M., Romanski, J., Ruedy, R., and Russell, G.: Drivers of Air-Sea CO_2 Flux Seasonality and its Long-Term Changes in the NASA-GISS model CMIP6 submission, J. Adv. Model. Earth Sy., 13, e2019MS002028, https://doi.org/10.1029/2019MS002028, 2021.

Leseurre, C., Lo Monaco, C., Reverdin, G., Metzl, N., Fin, J., Olafsdottir, S., and Racapé, V.: Ocean carbonate system variability in the North Atlantic Subpolar surface water (1993–2017), Biogeosciences, 17, 2553–2577, https://doi.org/10.5194/bg-17-2553-2020, 2020.

Leseurre, C., Lo Monaco, C., Reverdin, G., Metzl, N., Fin, J., Mignon, C., and Benito, L.: Summer trends and drivers of sea surface fCO_2 and pH changes observed in the southern Indian Ocean over the last two decades (1998–2019), Biogeosciences, 19, 2599–2625, https://doi.org/10.5194/bg-19-2599-2022, 2022.

Lherminier, P., Mercier, H., Gourcuff, C., Alvarez, M., Bacon, S., and Kermabon, C.: Transports across the 2002 Greenland-Portugal OVIDE section and comparison with 1997, J. Geophys. Res., 112, C07003, https://doi.org/10.1029/2006JC003716, 2007.

Li, B. F., Watanabe, Y. W., Hosoda, S., Sato, K., and Nakano, Y.: Quasireal-time and high-resolution spatiotemporal distribution of ocean anthropogenic CO_2, Geophys. Res. Lett., 46, 4836–4843, https://doi.org/10.1029/2018GL081639, 2019.

Lombard, F., Bourdin, G., Pesant, S., Agostini, S., Baudena, A., Boissin, E., Cassar, N., Clampitt, M., Conan, P., Da Silva, O., Dimier, C., Douville, E., Elineau, A., Fin, J., Flores, J.-M., Ghiglione, J.-F., Hume, B. C. C., Jalabert, L., John, S. G., Kelly, R. L., Koren, I., Lin, Y., Marie, D., McMinds, R., Mériguet, Z., Metzl, N., Paz-García, D. A., Luiza Pedrotti, M., Poulain, J., Pujo-Pay, M., Ras, J., Reverdin, G., Romac, S., Röttinger, E., Vardi, A., Voolstra, C. R., Moulin, C., Iwankow, G., Banaigs, B., Bowler, C., de Vargas, C., Forcioli, D., Furla, P., Galand, P. E., Gilson, E., Reynaud, S., Sunagawa, S., Thomas, O., Troublé, R., Vega Thurber, R., Wincker, P., Zoccola, D., Allemand, D., Planes, S., Boss, E., and Gorsky, G.: Open science resources from the Tara Pacific expedition across the surface ocean and coral reef ecosystems, Sci. Data, 10, 324, https://doi.org/10.1038/s41597-022-01757-w, 2023.

Lo Monaco, C., Álvarez, M., Key, R. M., Lin, X., Tanhua, T., Tilbrook, B., Bakker, D. C. E., van Heuven, S., Hoppema, M., Metzl, N., Ríos, A. F., Sabine, C. L., and Velo, A.: Assessing the internal consistency of the CARINA database in the Indian sector of the Southern Ocean, Earth Syst. Sci. Data, 2, 51–70, https://doi.org/10.5194/essd-2-51-2010, 2010.

Lo Monaco, C., Metzl, N., Fin, J., and Tribollet, A.: Sea surface measurements of dissolved inorganic carbon (DIC) and total alkalinity (TALK), temperature and salinity during the R/V Marion-Dufresne cruise CLIM-EPARSES (EXPOCODE 35MV20190405) in the Indian Ocean and Mozambique Channel from 2019-04-04 to 2019-04-30, NCEI Accession 0212218, NOAA National Centers for Environmental Information [data set] https://doi.org/10.25921/26rw-w185, 2020.

Lo Monaco, C., Metzl, N., Fin, J., Mignon, C., Cuet, P., Douville, E., Gehlen, M., Trang Chau, T. T., and Tribollet, A.: Distribution and long-term change of the sea surface carbonate system in the Mozambique Channel (1963–2019), Deep-Sea Res. Pt. II, 186–188, 104936, https://doi.org/10.1016/j.dsr2.2021.104936, 2021.

Lueker, T. J., Dickson, A. G., and Keeling, C. D.: Ocean pCO_2 calculated from dissolved inorganic carbon, alkalinity, and equations for K_1 and K_2: validation based on laboratory measurements of CO_2 in gas and seawater at equilibrium, Mar. Chem., 70, 105–119, https://doi.org/10.1016/S0304-4203(00)00022-0, 2000.

Ma, D., Gregor, L., and Gruber, N: Four decades of trends and drivers of global surface ocean acidification, Global Biogeochem. Cy., 37, e2023GB007765, https://doi.org/10.1029/2023GB007765, 2023.

Maier, C., Watremez, P., Taviani, M., Weinbauer, M. G., and Gattuso, J.-P.: Calcification rates and the effect of ocean acidification on Mediterranean cold-water corals, P. Roy. Soc. B-Biol. Sci., 279, 1716–1723, https://doi.org/10.1098/rspb.2011.1763, 2012.

Margirier, F., Testor, P., Heslop, E. Mallil, K., Bosse, A., Houpert, L., Mortier, L., Bouin, M.-N., Coppola, L., D'Ortenzio, F., Durrieu de Madron, X., Mourre, B., Prieur, L., Raimbault, P., and Taillandier, V.: Abrupt warming and salinification of intermediate waters interplays with decline of deep convection in the Northwestern Mediterranean Sea, Sci. Rep., 10, 20923, https://doi.org/10.1038/s41598-020-77859-5, 2020.

Marrec, P., Cariou, T., Collin, E., Durand, A., Latimier, M., Macé, E., Morin, P., Raimund, S., Vernet, M., and Bozec, Y.: Seasonal and latitudinal variability of the CO_2 system in the western English Channel based on Voluntary Observing Ship (VOS) measurements, Mar. Chem., 155, 29–41, 2013.

Marrec, P., Cariou, T., Latimier, M., Macé, E., Morin, P., Vernet, M., and Bozec, Y.: Spatio-temporal dynamics of biogeochemical processes and air–sea CO_2 fluxes in the Western English Channel based on two years of FerryBox deployment, J. Marine Syst., 140, 26–38, https://doi.org/10.1016/j.jmarsys.2014.05.010, 2014.

Marrec, P., Cariou, T., Macé, E., Morin, P., Salt, L. A., Vernet, M., Taylor, B., Paxman, K., and Bozec, Y.: Dynamics of air–sea CO_2 fluxes in the northwestern European shelf based on voluntary observing ship and satellite observations, Biogeosciences, 12, 5371–5391, https://doi.org/10.5194/bg-12-5371-2015, 2015.

Marrec, P. and Bozec, Y.: Partial pressure (or fugacity) of carbon dioxide, dissolved inorganic carbon, alkalinity and salinity collected from Surface underway observations using Carbon dioxide (CO_2) gas analyzer and other instruments from ARMORIQUE in the English Channel from 2012-04-25 to 2013-01-03 (NCEI Accession 0157472), Version 1.1, NOAA National Centers for Environmental Information [data set], https://doi.org/10.3334/CDIAC/OTG.COAST_FERRYBOX_ROSCOFF_PLYMOUTH_2012, 2016a.

Marrec, P. and Bozec, Y.: Partial pressure (or fugacity) of carbon dioxide, dissolved inorganic carbon, alkalinity and salinity collected from Surface underway observations using Carbon dioxide (CO_2) gas analyzer and other instruments from ARMORIQUE in the English Channel from 2013-03-15 to 2013-12-22 (NCEI Accession 0157444), Version 1.1, NOAA National Centers for Environmental Information [data set], https://doi.org/10.3334/CDIAC/OTG.COAST_FERRYBOX_ROSCOFF_PLYMOUTH_2013, 2016b.

Marrec, P. and Bozec, Y.: Partial pressure (or fugacity) of carbon dioxide, dissolved inorganic carbon, alkalinity and salinity collected from surface underway observations using Carbon dioxide (CO_2) gas analyzer and other instruments from ARMORIQUE in the English Channel from 2014-03-18 to 2014-10-09 (NCEI Accession 0163193), Version 1.1, NOAA National Centers for Environmental Information [data set], https://doi.org/10.3334/CDIAC/OTG.COAST_FERRYBOX_ROSCOFF_PLYMOUTH_2014, 2017.

Mazloff, M. R., Verdy, A., Gille, S. T., Johnson, K. S., Cornuelle, B. D., and Sarmiento, J.: Southern Ocean acidification revealed by biogeochemical-Argo floats, J. Geophys. Res.-Oceans, 128, e2022JC019530, https://doi.org/10.1029/2022JC019530, 2023.

McCulloch, M., Trotter, J., Montagna, P., Falter, J., Dunbar, R., Freiwald, A., Försterra, G., López Correa, M., Maier, C., Rüggeberg, A., and Taviani, M.: Resilience of cold-water scleractinian corals to ocean acidification: Boron isotopic systematics of pH and saturation state up-regulation, Geochim. Cosmochim. Ac., 87, 21–34, https://doi.org/10.1016/j.gca.2012.03.027, 2012.

McKinley, G. A., Fay, A. R., Takahashi, T., and Metzl, N.: Convergence of atmospheric and North Atlantic carbon dioxide trends on multidecadal timescales, Nat. Geosci., 4, 606–610, https://doi.org/10.1038/NGEO1193, 2011.

McKinley, G. A., Ritzer, A. L., and Lovenduski, N. S.: Mechanisms of northern North Atlantic biomass variability, Biogeosciences, 15, 6049–6066, https://doi.org/10.5194/bg-15-6049-2018, 2018.

Meier, K. J. S., Beaufort, L., Heussner, S., and Ziveri, P.: The role of ocean acidification in *Emiliania huxleyi* coccolith thinning in the Mediterranean Sea, Biogeosciences, 11, 2857–2869, https://doi.org/10.5194/bg-11-2857-2014, 2014.

Mercier, H., Lherminier, P., Sarafanov, A., Gaillard, F., Daniault, N., Desbruyères, D., Falina, A., Ferron, B., Huck, T., and Thierry, V.: Variability of the meridional overturning circulation at the Greenland-Portugal Ovide section from 1993 to 2010, Prog. Oceanogr., 132, 250–261, https://doi.org/10.1016/j.pocean.2013.11.001, 2015.

Merlivat, L., Boutin, J., Antoine, D., Beaumont, L., Golbol, M., and Vellucci, V.: Increase of dissolved inorganic carbon and decrease in pH in near-surface waters in the Mediterranean Sea during the past two decades, Biogeosciences, 15, 5653–5662, https://doi.org/10.5194/bg-15-5653-2018, 2018.

Metzl, N., Brunet, C., Jabaud-Jan, A., Poisson, A., and Schauer, B.: Summer and winter air-sea CO_2 fluxes in the Southern Ocean, Deep-Sea Res. Pt. I, 53, 1548–1563, https://doi.org/10.1016/j.dsr.2006.07.006, 2006.

Metzl, N., Tilbrook, B., Bakker, D., Le Quéré, C., Doney, S., Feely, R., Hood M., and Dargaville, R.: Global Changes in Ocean Carbon: Variability and Vulnerability, Eos, 88, 286–287, https://doi.org/10.1029/2007EO280005, 2007.

Metzl, N., Corbière, A., Reverdin, G., Lenton, A., Takahashi, T., Olsen, A., Johannessen, T., Pierrot, D., Wanninkhof, R., Ólafsdóttir, S. R., Olafsson, J., and Ramonet, M.: Recent acceleration of the sea surface fCO_2 growth rate in the North Atlantic subpolar gyre (1993–2008) revealed by winter observations, Global Biogeochem. Cy., 24, GB4004, https://doi.org/10.1029/2009GB003658, 2010.

Metzl, N., Ferron, B., Lherminier, P., Sarthou, G., and Thierry, V.: Discrete profile measurements of dissolved inorganic carbon (DIC), total alkalinity (TALK), temperature and salinity during the multiple ships Observatoire de la variabilité interannuelle et décennale en Atlantique Nord (OVIDE) project, OVIDE-2006, OVIDE-2008, OVIDE-2010, OVIDE-2012, OVIDE-2014 cruises in the North Atlantic Ocean from 2006-05-23 to 2014-06-30 (NCEI Accession 0177219), Version 1.1, NOAA National Centers for Environmental Information [data set], https://doi.org/10.25921/v0qt-ms48, 2018.

Metzl, N., Fin, J., Lo Monaco, C., et al.: A synthesis of total alkalinity and dissolved inorganic carbon measurements in the global ocean (1993–2022) SNAPO-CO2-V1 dataset, SEANOE [data set], https://doi.org/10.17882/95414, 2023.

Mignot, A., Claustre, H., Cossarini, G., D'Ortenzio, F., Gutknecht, E., Lamouroux, J., Lazzari, P., Perruche, C., Salon, S., Sauzède, R., Taillandier, V., and Teruzzi, A.: Using machine learning and Biogeochemical-Argo (BGC-Argo) floats to assess biogeochemical models and optimize observing system design, Biogeosciences, 20, 1405–1422, https://doi.org/10.5194/bg-20-1405-2023, 2023.

Millero, F. J., Lee, K., and Roche, M.: Distribution of alkalinity in the surface waters of the major oceans, Mar. Chem., 60, 111–130, https://doi.org/10.1016/S0304-4203(97)00084-4, 1998.

Mongwe, N. P., Vichi, M., and Monteiro, P. M. S.: The seasonal cycle of pCO_2 and CO_2 fluxes in the Southern Ocean: diagnosing anomalies in CMIP5 Earth system models, Biogeosciences, 15, 2851–2872, https://doi.org/10.5194/bg-15-2851-2018, 2018.

Moutin, T., Wagener, T., Caffin, M., Fumenia, A., Gimenez, A., Baklouti, M., Bouruet-Aubertot, P., Pujo-Pay, M., Leblanc, K., Lefevre, D., Helias Nunige, S., Leblond, N., Grosso, O., and de Verneil, A.: Nutrient availability and the ultimate control of the biological carbon pump in the western tropical South Pacific Ocean, Biogeosciences, 15, 2961–2989, https://doi.org/10.5194/bg-15-2961-2018, 2018.

Newton, J. A., Feely, R. A., Jewett, E. B., Williamson, P., and Mathis, J.: Global Ocean Acidification Observing Network: Requirements and Governance Plan. Second Edition, GOA-ON, https://www.iaea.org/sites/default/files/18/06/goa-on-second-edition-2015.pdf (last access: 22 December 2023), 2015.

Nykjaer, L.: Mediterranean Sea surface warming 1985–2006, Clim. Res., 39, 11–17, https://doi.org/10.3354/cr00794, 2009.

OCADS: Coastal Carbon Data, https://www.ncei.noaa.gov/access/ocean-carbon-acidification-data-system/oceans/coastal_carbon_data.html, last access: 22 December 2023.

Olafsson, J., Olafsdottir, S. R., Benoit-Cattin, A., Danielsen, M., Arnarson, T. S., and Takahashi, T.: Rate of Iceland Sea acidification from time series measurements, Biogeosciences, 6, 2661–2668, https://doi.org/10.5194/bg-6-2661-2009, 2009.

Olivier, L., Boutin, J., Reverdin, G., Lefèvre, N., Landschützer, P., Speich, S., Karstensen, J., Labaste, M., Noisel, C., Ritschel, M., Steinhoff, T., and Wanninkhof, R.: Wintertime process study of the North Brazil Current rings reveals the region as a larger sink for CO_2 than expected, Biogeosciences, 19, 2969–2988, https://doi.org/10.5194/bg-19-2969-2022, 2022.

Olsen, A., Key, R. M., van Heuven, S., Lauvset, S. K., Velo, A., Lin, X., Schirnick, C., Kozyr, A., Tanhua, T., Hoppema, M., Jutterström, S., Steinfeldt, R., Jeansson, E., Ishii, M., Pérez, F. F., and Suzuki, T.: The Global Ocean Data Analysis Project version 2 (GLODAPv2) – an internally consistent data product for the world ocean, Earth Syst. Sci. Data, 8, 297–323, https://doi.org/10.5194/essd-8-297-2016, 2016.

Olsen, A., Lange, N., Key, R. M., Tanhua, T., Álvarez, M., Becker, S., Bittig, H. C., Carter, B. R., Cotrim da Cunha, L., Feely, R. A., van Heuven, S., Hoppema, M., Ishii, M., Jeansson, E., Jones, S. D., Jutterström, S., Karlsen, M. K., Kozyr, A., Lauvset, S. K., Lo Monaco, C., Murata, A., Pérez, F. F., Pfeil, B., Schirnick, C., Steinfeldt, R., Suzuki, T., Telszewski, M., Tilbrook, B., Velo, A., and Wanninkhof, R.: GLODAPv2.2019 – an update of GLODAPv2, Earth Syst. Sci. Data, 11, 1437–1461, https://doi.org/10.5194/essd-11-1437-2019, 2019.

Olsen, A., Lange, N., Key, R. M., Tanhua, T., Bittig, H. C., Kozyr, A., Álvarez, M., Azetsu-Scott, K., Becker, S., Brown, P. J., Carter, B. R., Cotrim da Cunha, L., Feely, R. A., van Heuven, S., Hoppema, M., Ishii, M., Jeansson, E., Jutterström, S., Landa, C. S., Lauvset, S. K., Michaelis, P., Murata, A., Pérez, F. F., Pfeil, B., Schirnick, C., Steinfeldt, R., Suzuki, T., Tilbrook, B., Velo, A., Wanninkhof, R., and Woosley, R. J.: An updated version of the global interior ocean biogeochemical data product, GLODAPv2.2020, Earth Syst. Sci. Data, 12, 3653–3678, https://doi.org/10.5194/essd-12-3653-2020, 2020.

Orr, J. C., Epitalon, J.-M., and Gattuso, J.-P.: Comparison of ten packages that compute ocean carbonate chemistry, Biogeosciences, 12, 1483–1510, https://doi.org/10.5194/bg-12-1483-2015, 2015.

Orr, J. C., Epitalon, J.-M., Dickson, A. G., and Gattuso, J.-P.: Routine uncertainty propagation for the marine carbon dioxide system, Mar. Chem., 207, 84–107, https://doi.org/10.1016/j.marchem.2018.10.006, 2018.

Parard, G., Lefèvre, N., and Boutin, J.: Sea water fugacity of CO_2 at the PIRATA mooring at 6° S, 10° W, Tellus B, 62, 636–648, https://doi.org/10.1111/j.1600-0889.2010.00503.x, 2010.

Pérez, F. F., Vázquez-Rodríguez, M., Mercier, H., Velo, A., Lherminier, P., and Ríos, A. F.: Trends of anthropogenic CO_2 storage in North Atlantic water masses, Biogeosciences, 7, 1789–1807, https://doi.org/10.5194/bg-7-1789-2010, 2010.

Pérez, F. F., Mercier, H., Vazquez-Rodriguez, M., Lherminier, P., Velo, A., Pardo, P., Roson, G., and Rios, A.: Reconciling air-sea CO_2 fluxes and anthropogenic CO_2 budgets in a changing North Atlantic, Nat. Geosci., 6, 146–152, https://doi.org/10.1038/ngeo1680, 2013.

Pérez, F., Fontela, M., García-Ibáñez, M., Mercier, H., Velo, A., Lherminier, P., Zunino, P., de la Paz, M., Alonso-Pérez, F., Guallart, E. F., and Padin, X. A.: Meridional overturning circulation conveys fast acidification to the deep Atlantic Ocean, Nature, 554, 515–518, https://doi.org/10.1038/nature25493, 2018.

Petrenko, A. A., Doglioli, A. M., Nencioli, F., Kersalé, M., Hu, Z., and d'Ovidio, F.: A review of the LATEX project: mesoscale to submesoscale processes in a coastal environment, Ocean Dy-

nam., 67, 513–533, https://doi.org/10.1007/s10236-017-1040-9, 2017.

Petton, S., Pouvreau, S., and Fleury, E.: ECOSCOPA network: high frequency environmental databasem SEANOE [data set], https://doi.org/10.17882/86131, 2023.

Pfeil, B., Olsen, A., Bakker, D. C. E., Hankin, S., Koyuk, H., Kozyr, A., Malczyk, J., Manke, A., Metzl, N., Sabine, C. L., Akl, J., Alin, S. R., Bates, N., Bellerby, R. G. J., Borges, A., Boutin, J., Brown, P. J., Cai, W.-J., Chavez, F. P., Chen, A., Cosca, C., Fassbender, A. J., Feely, R. A., González-Dávila, M., Goyet, C., Hales, B., Hardman-Mountford, N., Heinze, C., Hood, M., Hoppema, M., Hunt, C. W., Hydes, D., Ishii, M., Johannessen, T., Jones, S. D., Key, R. M., Körtzinger, A., Landschützer, P., Lauvset, S. K., Lefèvre, N., Lenton, A., Lourantou, A., Merlivat, L., Midorikawa, T., Mintrop, L., Miyazaki, C., Murata, A., Nakadate, A., Nakano, Y., Nakaoka, S., Nojiri, Y., Omar, A. M., Padin, X. A., Park, G.-H., Paterson, K., Perez, F. F., Pierrot, D., Poisson, A., Ríos, A. F., Santana-Casiano, J. M., Salisbury, J., Sarma, V. V. S. S., Schlitzer, R., Schneider, B., Schuster, U., Sieger, R., Skjelvan, I., Steinhoff, T., Suzuki, T., Takahashi, T., Tedesco, K., Telszewski, M., Thomas, H., Tilbrook, B., Tjiputra, J., Vandemark, D., Veness, T., Wanninkhof, R., Watson, A. J., Weiss, R., Wong, C. S., and Yoshikawa-Inoue, H.: A uniform, quality controlled Surface Ocean CO_2 Atlas (SOCAT), Earth Syst. Sci. Data, 5, 125–143, https://doi.org/10.5194/essd-5-125-2013, 2013.

Pilcher, D. J., Brody, S. R., Johnson, L., and Bronselaer, B.: Assessing the abilities of CMIP5 models to represent the seasonal cycle of surface ocean pCO_2, J. Geophys. Res.-Oceans, 120, 4625–4637, https://doi.org/10.1002/2015JC010759, 2015.

Poisson, A., Culkin, F., and Ridout, P.: Intercomparison of CO_2 measurements, Deep-Sea Res. Pt. I, 37, 1647–1650, https://doi.org/10.1016/0198-0149(90)90067-6, 1990.

Racapé, V., Metzl, N., Pierre, C., Reverdin, G., Quay, P. D., and Olafsdottir, S. R.: The seasonal cycle of δ^3CDIC in the North Atlantic subpolar gyre, Biogeosciences, 11, 1683–1692, https://doi.org/10.5194/bg-11-1683-2014, 2014.

Revelle, R. and Suess, H. E.: Carbon dioxide exchange between atmosphere and ocean and the question of an increase of atmospheric CO_2 during the past decades, Tellus, 9, 18–27, https://doi.org/10.1111/j.2153-3490.1957.tb01849.x, 1957.

Reverdin, G., Metzl, N., Olafsdottir, S., Racapé, V., Takahashi, T., Benetti, M., Valdimarsson, H., Benoit-Cattin, A., Danielsen, M., Fin, J., Naamar, A., Pierrot, D., Sullivan, K., Bringas, F., and Goni, G.: SURATLANT: a 1993–2017 surface sampling in the central part of the North Atlantic subpolar gyre, Earth Syst. Sci. Data, 10, 1901–1924, https://doi.org/10.5194/essd-10-1901-2018, 2018.

Ridame, C., Dekaezemacker, J., Guieu, C., Bonnet, S., L'Helguen, S., and Malien, F.: Contrasted Saharan dust events in LNLC environments: impact on nutrient dynamics and primary production, Biogeosciences, 11, 4783–4800, https://doi.org/10.5194/bg-11-4783-2014, 2014.

Robertson, J. E., Robinson, C., Turner, D. R., Holligan, P., Watson, A. J., Boyd, P., Fernandez, E., and Finch, M.: The impact of a coccolithophore bloom on oceanic carbon uptake in the northeast Atlantic during summer 1991, Deep-Sea Res. Pt. I, 41, 297–314, 1994.

Rödenbeck, C., Keeling, R. F., Bakker, D. C. E., Metzl, N., Olsen, A., Sabine, C., and Heimann, M.: Global surface-ocean pCO_2 and sea–air CO_2 flux variability from an observation-driven ocean mixed-layer scheme, Ocean Sci., 9, 193–216, https://doi.org/10.5194/os-9-193-2013, 2013.

Rödenbeck, C., Bakker, D. C. E., Gruber, N., Iida, Y., Jacobson, A. R., Jones, S., Landschützer, P., Metzl, N., Nakaoka, S., Olsen, A., Park, G.-H., Peylin, P., Rodgers, K. B., Sasse, T. P., Schuster, U., Shutler, J. D., Valsala, V., Wanninkhof, R., and Zeng, J.: Data-based estimates of the ocean carbon sink variability – first results of the Surface Ocean pCO_2 Mapping intercomparison (SOCOM), Biogeosciences, 12, 7251–7278, https://doi.org/10.5194/bg-12-7251-2015, 2015.

Sabine, C. L., Feely, R. A., Gruber, N., Key, R. M., Lee, K., Bullister, J. L., Wanninkhof, R., Wong, C. S., Wallace, D. W. R., Tilbrook, B., Millero, F. J., Peng, T.-H., Kozyr, A., Ono, T., and Rios, A. F.: The Oceanic Sink for Anthropogenic CO_2, Science, 305, 367–371, https://doi.org/10.1126/science.1097403, 2004.

Sabine, C. L., Hankin, S., Koyuk, H., Bakker, D. C. E., Pfeil, B., Olsen, A., Metzl, N., Kozyr, A., Fassbender, A., Manke, A., Malczyk, J., Akl, J., Alin, S. R., Bellerby, R. G. J., Borges, A., Boutin, J., Brown, P. J., Cai, W.-J., Chavez, F. P., Chen, A., Cosca, C., Feely, R. A., González-Dávila, M., Goyet, C., Hardman-Mountford, N., Heinze, C., Hoppema, M., Hunt, C. W., Hydes, D., Ishii, M., Johannessen, T., Key, R. M., Körtzinger, A., Landschützer, P., Lauvset, S. K., Lefèvre, N., Lenton, A., Lourantou, A., Merlivat, L., Midorikawa, T., Mintrop, L., Miyazaki, C., Murata, A., Nakadate, A., Nakano, Y., Nakaoka, S., Nojiri, Y., Omar, A. M., Padin, X. A., Park, G.-H., Paterson, K., Perez, F. F., Pierrot, D., Poisson, A., Ríos, A. F., Salisbury, J., Santana-Casiano, J. M., Sarma, V. V. S. S., Schlitzer, R., Schneider, B., Schuster, U., Sieger, R., Skjelvan, I., Steinhoff, T., Suzuki, T., Takahashi, T., Tedesco, K., Telszewski, M., Thomas, H., Tilbrook, B., Vandemark, D., Veness, T., Watson, A. J., Weiss, R., Wong, C. S., and Yoshikawa-Inoue, H.: Surface Ocean CO_2 Atlas (SOCAT) gridded data products, Earth Syst. Sci. Data, 5, 145–153, https://doi.org/10.5194/essd-5-145-2013, 2013.

Salt, L. A., Beaumont, L., Blain, S., Bucciarelli, E., Grosstefan, E., Guillot, A., L'Helguen, S., Merlivat, L., Répécaud, M., Quéméner, L., Rimmelin-Maury, P., Tréguer, P., and Bozec, Y.: The annual and seasonal variability of the carbonate system in the Bay of Brest (Northwest Atlantic Shelf, 2008–2014), Mar. Chem., 187, 1–15, https://doi.org/10.1016/j.marchem.2016.09.003, 2016.

Sasse, T. P., McNeil, B. I., and Abramowitz, G.: A novel method for diagnosing seasonal to inter-annual surface ocean carbon dynamics from bottle data using neural networks, Biogeosciences, 10, 4319–4340, https://doi.org/10.5194/bg-10-4319-2013, 2013.

Sauzède, R., Claustre, H., Pasqueron de Fommervault, O., Bittig, H., Gattuso, J.-P., Legendre, L., and Johnson, K. S.: Estimates of water-column nutrients and carbonate system parameters in the global ocean: A novel approach based on neural networks, Front. Mar. Sci., 4, 128, https://doi.org/10.3389/fmars.2017.00128, 2017.

Schlitzer, R.: Ocean Data View, http://odv.awi.de (last access: 13 March 2019), 2018.

Schneider, A., Wallace, D. W. R., and Körtzinger, A.: Alkalinity of the Mediterranean Sea, Geophys. Res. Lett., 34, L15608, https://doi.org/10.1029/2006GL028842, 2007.

Schuster, U., Watson, A. J., Bates, N., Corbière, A., Gonzalez-Davila, M., Metzl, N., Pierrot, D., and Santana-Casiano, M.: Trends in North Atlantic sea surface pCO_2 from 1990 to 2006, Deep-Sea Res. Pt. II, 56, 620–629, https://doi.org/10.1016/j.dsr2.2008.12.011, 2009.

Schuster, U., McKinley, G. A., Bates, N., Chevallier, F., Doney, S. C., Fay, A. R., González-Dávila, M., Gruber, N., Jones, S., Krijnen, J., Landschützer, P., Lefèvre, N., Manizza, M., Mathis, J., Metzl, N., Olsen, A., Rios, A. F., Rödenbeck, C., Santana-Casiano, J. M., Takahashi, T., Wanninkhof, R., and Watson, A. J.: An assessment of the Atlantic and Arctic sea–air CO_2 fluxes, 1990–2009, Biogeosciences, 10, 607–627, https://doi.org/10.5194/bg-10-607-2013, 2013.

Seelmann, K., Steinhoff, T., Aßmann, S., and Körtzinger, A.:. Enhance Ocean Carbon Observations: Successful Implementation of a Novel Autonomous Total Alkalinity Analyzer on a Ship of Opportunity, Front. Mar. Sci., 7, 571301, https://doi.org/10.3389/fmars.2020.571301, 2020.

Sims, R. P., Holding, T. M., Land, P. E., Piolle, J.-F., Green, H. L., and Shutler, J. D.: OceanSODA-UNEXE: a multi-year gridded Amazon and Congo River outflow surface ocean carbonate system dataset, Earth Syst. Sci. Data, 15, 2499–2516, https://doi.org/10.5194/essd-15-2499-2023, 2023.

Skjelvan, I., Lauvset, S. K., Johannessen, T., Gundersen, K., and Skagseth, Ø.: Decadal trends in Ocean Acidification from the Ocean Weather Station M in the Norwegian Sea, J. Marine Syst., 234, 103775, https://doi.org/10.1016/j.jmarsys.2022.103775, 2022.

Takahashi, T., Sutherland, S. C., Sweeney, C., Poisson, A., Metzl, N., Tilbrook, B., Bates, N., Wanninkhof, R., Feely, R. A., Sabine, C., Olafsson, J., and Nojiri, Y.: Global Sea-Air CO_2 Flux Based on Climatological Surface Ocean pCO_2, and Seasonal Biological and Temperature Effect, Deep-Sea Res. Pt. II, 49, 1601–1622, https://doi.org/10.1016/S0967-0645(02)00003-6, 2002.

Takahashi, T., Sutherland, S. C., Wanninkhof, R., Sweeney, C., Feely, R. A., Chipman, D. W., Hales, B., Friederich, G., Chavez, F., Sabine, C., Watson, A. J., Bakker, D. C., Schuster, U., Metzl, N., Yoshikawa-Inoue, H., Ishii, M., Midorikawa, T., Nojiri, Y., Körtzinger, A., Steinhoff, T., Hoppema, M., Olafsson, J., Arnarson, T. S., Tilbrook, B., Johannessen, T., Olsen, A., Bellerby, R., Wong, C., Delille, B., Bates, N., and de Baar, H. J.: Climatological mean and decadal change in surface ocean pCO_2, and net sea air CO_2 flux over the global oceans, Deep-Sea Res. Pt. II, 56, 554–577, https://doi.org/10.1016/j.dsr2.2008.12.009, 2009.

Takahashi, T., Sutherland, S. C., Chipman, D. W., Goddard, J. G., Ho, C., Newberger, T., Sweeney, C., and Munro, D. R.: Climatological distributions of pH, pCO_2, total CO_2, alkalinity, and $CaCO_3$ saturation in the global surface ocean, and temporal changes at selected locations, Mar. Chem., 164, 95–125, https://doi.org/10.1016/j.marchem.2014.06.004, 2014.

Tanhua, T., Pouliquen, S., Hausman, J., O'Brien, K., Bricher, P., de Bruin, T., Buck, J. J. H., Burger, E. F., Carval, T., Casey, K. S., Diggs, S., Giorgetti, A., Glaves, H., Harscoat, V., Kinkade, D., Muelbert, J. H., Novellino, A., Pfeil, B., Pulsifer, P. L., Van de Putte, A., Robinson, E., Schaap, D., Smirnov, A., Smith, N., Snowden, D., Spears, T., Stall, S., Tacoma, M., Thijsse, P., Tronstad, S., Vandenberghe, T., Wengren, M., Wyborn, L., and Zhao, Z.: Ocean FAIR Data Services, Front. Mar. Sci., 6, 440, https://doi.org/10.3389/fmars.2019.00440, 2019.

Tanhua, T., Lauvset, S. K., Lange, N. et al.: A vision for FAIR ocean data products, Commun. Earth Environ., 2, 136, https://doi.org/10.1038/s43247-021-00209-4, 2021.

Testor, P., Bosse, A., and Coppola, L.: MOOSE-GE, https://doi.org/10.18142/235, 2010.

Tilbrook, B., Jewett, E. B., DeGrandpre, M. D., Hernandez-Ayon, J. M., Feely, R. A., Gledhill, D. K., Hansson, L., Isensee, K., Kurz, M. L., Newton, J. A., Siedlecki, S. A., Chai, F., Dupont, S., Graco, M., Calvo, E., Greeley, D., Kapsenberg, L., Lebrec, M., Pelejero, C., Schoo, K. L., and Telszewski, M.: An Enhanced Ocean Acidification Observing Network: From People to Technology to Data Synthesis and Information Exchange, Front. Mar. Sci., 6, 337, https://doi.org/10.3389/fmars.2019.00337, 2019.

Touratier, F., and Goyet, C.: Decadal evolution of anthropogenic CO_2 in the north western Mediterranean Sea from the mid-1990's to the mid-2000's, Deep-Sea Res. Pt I, 56, 1708–1716, https://doi.org/10.1016/j.dsr.2009.05.015, 2009.

Touratier, F., Azouzi, L., and Goyet, C.: CFC-11, $\Delta^{14}C$ and ^{3}H tracers as a means to assess anthropogenic CO_2 concentrations in the ocean, Tellus B, 59, 318–325, https://doi.org/10.1111/j.1600-0889.2006.00247.x, 2007.

Touratier, F., Goyet, C., Houpert, L., Durrieu de Madron, X., Lefèvre, D., Stabholz, M., and Guglielmi, V.: Role of deep convection on anthropogenic CO_2 sequestration in the Gulf of Lions (northwestern Mediterranean Sea), Deep-Sea Res. Pt. I, 113, 33–48, https://doi.org/10.1016/j.dsr.2016.04.003, 2016.

Turk, D., Dowd, M., Lauvset, S. K., Koelling, J., Alonso-Pérez, F., and Pérez, F. F.: Can Empirical Algorithms Successfully Estimate Aragonite Saturation State in the Subpolar North Atlantic?, Front. Mar. Sci., 4, 385, https://doi.org/10.3389/fmars.2017.00385, 2017.

UNESCO: Intercomparison of total alkalinity and total inorganic carbon determinations in seawater, UNESCO Tech. Pap. Mar. Sci., 59, https://www.jodc.go.jp/jodcweb/info/ioc_doc/UNESCO_tech/090199eb.pdf (last access: 22 December 2023), 1990.

UNESCO: Reference materials for oceanic carbon dioxide measurements, UNESCO Tech. Pap. Mar. Sci., 60, https://www.jodc.go.jp/jodcweb/info/ioc_doc/UNESCO_tech/090200eb.pdf (last access: 22 December 2023), 1991.

United Nations: The Sustainable Development Goals 2020, 68 pp. https://unstats.un.org/sdgs/report/2020/ (last access: 22 December 2023), 2020.

Vangriesheim A., Pierre, C., Aminot, A., Metzl, N., Baurand, F., and Caprais, J.-C.: The influence of Congo river discharges in the surface and deep layers of the Gulf of Guinea, Deep-Sea Res. Pt. II, https://doi.org/10.1016/j.dsr2.2009.04.002, 2009.

Vázquez-Rodríguez, M., Pérez, F. F., Velo, A., Ríos, A. F., and Mercier, H.: Observed acidification trends in North Atlantic water masses, Biogeosciences, 9, 5217–5230, https://doi.org/10.5194/bg-9-5217-2012, 2012.

Velo, A., Perez, F. F., Brown, P., Tanhua, T., Schuster, U., and Key, R. M.: CARINA alkalinity data in the Atlantic Ocean, Earth Syst. Sci. Data, 1, 45–61, https://doi.org/10.5194/essd-1-45-2009, 2009.

von Schuckmann, K., Cheng, L., Palmer, M. D., Hansen, J., Tassone, C., Aich, V., Adusumilli, S., Beltrami, H., Boyer, T., Cuesta-Valero, F. J., Desbruyères, D., Domingues, C., García-García, A., Gentine, P., Gilson, J., Gorfer, M., Haim-

berger, L., Ishii, M., Johnson, G. C., Killick, R., King, B. A., Kirchengast, G., Kolodziejczyk, N., Lyman, J., Marzeion, B., Mayer, M., Monier, M., Monselesan, D. P., Purkey, S., Roemmich, D., Schweiger, A., Seneviratne, S. I., Shepherd, A., Slater, D. A., Steiner, A. K., Straneo, F., Timmermans, M.-L., and Wijffels, S. E.: Heat stored in the Earth system: where does the energy go?, Earth Syst. Sci. Data, 12, 2013–2041, https://doi.org/10.5194/essd-12-2013-2020, 2020.

von Schuckmann, K., Minière, A., Gues, F., Cuesta-Valero, F. J., Kirchengast, G., Adusumilli, S., Straneo, F., Ablain, M., Allan, R. P., Barker, P. M., Beltrami, H., Blazquez, A., Boyer, T., Cheng, L., Church, J., Desbruyeres, D., Dolman, H., Domingues, C. M., García-García, A., Giglio, D., Gilson, J. E., Gorfer, M., Haimberger, L., Hakuba, M. Z., Hendricks, S., Hosoda, S., Johnson, G. C., Killick, R., King, B., Kolodziejczyk, N., Korosov, A., Krinner, G., Kuusela, M., Landerer, F. W., Langer, M., Lavergne, T., Lawrence, I., Li, Y., Lyman, J., Marti, F., Marzeion, B., Mayer, M., MacDougall, A. H., McDougall, T., Monselesan, D. P., Nitzbon, J., Otosaka, I., Peng, J., Purkey, S., Roemmich, D., Sato, K., Sato, K., Savita, A., Schweiger, A., Shepherd, A., Seneviratne, S. I., Simons, L., Slater, D. A., Slater, T., Steiner, A. K., Suga, T., Szekely, T., Thiery, W., Timmermans, M.-L., Vanderkelen, I., Wjiffels, S. E., Wu, T., and Zemp, M.: Heat stored in the Earth system 1960–2020: where does the energy go?, Earth Syst. Sci. Data, 15, 1675–1709, https://doi.org/10.5194/essd-15-1675-2023, 2023.

Wagener, T., Metzl, N., Caffin, M., Fin, J., Helias Nunige, S., Lefevre, D., Lo Monaco, C., Rougier, G., and Moutin, T.: Carbonate system distribution, anthropogenic carbon and acidification in the western tropical South Pacific (OUTPACE 2015 transect), Biogeosciences, 15, 5221–5236, https://doi.org/10.5194/bg-15-5221-2018, 2018a.

Wagener, T., Metzl, N., Caffin, M., Fin, J., Helias Nunige, S., Lefèvre, D., Lo Monaco, C., Rougier, G., and Moutin, T.: Discrete profile measurements of dissolved inorganic carbon (DIC), total alkalinity (TALK), temperature, salinity and other parameters during the R/V L'Atalante "Oligotrophy from UltraoligoTrophy PACific Experiment" (OUTPACE) cruise (EXPOCODE 35A320150218) in the South Pacific Ocean from 2015-02-18 to 2015-04-03 (NCEI Accession 0177706), Version 1.1, NOAA National Centers for Environmental Information [data set], https://doi.org/10.25921/wbkb-0q19, 2018b.

Walton, D. W. H. and Thomas, J.: Cruise Report – Antarctic Circumnavigation Expedition (ACE) 20th December 2016–19th March 2017 (1.0), Zenodo [data set], https://doi.org/10.5281/zenodo.1443511, 2018.

Wanninkhof, R., Park, G.-H., Takahashi, T., Sweeney, C., Feely, R., Nojiri, Y., Gruber, N., Doney, S. C., McKinley, G. A., Lenton, A., Le Quéré, C., Heinze, C., Schwinger, J., Graven, H., and Khatiwala, S.: Global ocean carbon uptake: magnitude, variability and trends, Biogeosciences, 10, 1983–2000, https://doi.org/10.5194/bg-10-1983-2013, 2013.

Watson, A. J., Schuster, U., Bakker, D. C. E., Bates, N., Corbiere, A., Gonzalez-Davila, M., Freidrich, T., Hauck, J., Heinze, C., Johannessen, T., Koertzinger, A., Metzl, N., Olafsson, J., Olsen, A., Oschlies, A., Padin, X., Pfeil, B., Rios, A., Santana-Casiano, M, Steinhoff, T., Telszewski, M., Wallace, D. W. R., and Wanninkhof, R.: Tracking the variable North Atlantic sink for atmospheric CO_2, Science, 326, 1391, https://doi.org/10.1126/science.1177394, 2009.

Watson, A. J., Schuster, U., Shutler, J. D., Holding, T., Ashton, I. G. C., Landschützer, P., Woolf, D. K., and Goddijn-Murphy, L.: Revised estimates of ocean-atmosphere CO_2 flux are consistent with ocean carbon inventory, Nat. Commun., 11, 4422, https://doi.org/10.1038/s41467-020-18203-3, 2020.

Williams, N. L., Juranek, L. W., Johnson, K. S., Feely, R. A., Riser, S. C., Talley, L. D., Russell, J. L., Sarmiento, J. L., and Wanninkhof, R.: Empirical algorithms to estimate water column pH in the Southern Ocean, Geophys. Res. Lett., 43, 3415–3422, https://doi.org/10.1002/2016GL068539, 2016.

Williams, N. L., Juranek, L. W., Feely, R. A., Johnson, K. S., Sarmiento, J. L., Talley, L. D., Dickson, A. G., Gray, A. R., Wanninkhof, R., Russell, J. L., Riser, S. C., and Takeshita, Y.: Calculating surface ocean pCO_2 from biogeochemical Argo floats equipped with pH: An uncertainty analysis, Global Biogeochem. Cy., 31, 591–604, https://doi.org/10.1002/2016GB005541, 2017.

Williams, N. L., Juranek, L. W., Feely, R. A., Russell, J. L., Johnson, K. S., and Hales, B.: Assessment of the carbonate chemistry seasonal cycles in the Southern Ocean from persistent observational platforms, J. Geophys. Res.-Oceans, 123, 4833–4852, https://doi.org/10.1029/2017JC012917, 2018.

Wimart-Rousseau, C., Lajaunie-Salla, K., Marrec, P., Wagener, T., Raimbault, P., Lagadec, V., Lafont, M., Garcia, N., Diaz, F., Pinazo, C., Yohia, C., Garcia, F., Xueref-Remy, I., Blanc, P.-E., Armengaud, A., and Lefèvre, D.: Temporal variability of the carbonate system and air-sea CO_2 exchanges in a Mediterranean human-impacted coastal site, Estuar. Coast. Shelf S., 236, 106641, https://doi.org/10.1016/j.ecss.2020.106641, 2020.

Wimart-Rousseau, C., Wagener, T., Álvarez, M., Moutin, T., Fourrier, M., Coppola, L., Niclas-Chirurgien, L., Raimbault, P., D'Ortenzio, F., Durrieu de Madron, X., Taillandier, V., Dumas, F., Conan, P., Pujo-Pay, M., and Lefèvre, D.: Seasonal and Interannual Variability of the CO_2 System in the Eastern Mediterranean Sea: A Case Study in the North Western Levantine Basin, Front. Mar. Sci., 8, 649246, https://doi.org/10.3389/fmars.2021.649246, 2021.

WMO/GCOS: Global Climate Indicators, https://gcos.wmo.int/en/global-climate-indicators (last access: 22 December 2023), 2018.

Wu, Y., Hain, M. P., Humphreys, M. P., Hartman, S., and Tyrrell, T.: What drives the latitudinal gradient in open-ocean surface dissolved inorganic carbon concentration?, Biogeosciences, 16, 2661–2681, https://doi.org/10.5194/bg-16-2661-2019, 2019.